per unit length (i.e. $dB\,km^{-1}$) following:

$$\alpha_{dB}L = 10 \log_{10} \frac{P_i}{P_o} \tag{3.3}$$

where α_{dB} is the signal attenuation per unit length in decibels and L is the fiber length

---

Example 3.1

When the mean optical power launched into an 8 km length of fiber is 120 μW, the mean optical power at the fiber output is 3 μW.

Determine:

(a) the overall signal attenuation or loss in decibels through the fiber assuming there are no connectors or splices;
(b) the signal attenuation per kilometre for the fiber.
(c) the overall signal attenuation for a 10 km optical link using the same fiber with splices at 1 km intervals, each giving an attenuation of 1 dB;
(d) the numerical input/output power ratio in (c).

Solution: (a) Using Eq. (3.1), the overall signal attenuation in decibels through the fiber is:

$$\textit{Signal attenuation} = 10 \log_{10} \frac{P_i}{P_o} = 10 \log_{10} \frac{120 \times 10^{-6}}{3 \times 10^{-6}}$$

$$= 10 \log_{10} 40 = 16.0 \text{ dB}$$

(b) The signal attenuation per kilometre for the fiber may be simply obtained by dividing the result in (a) by the fiber length which corresponds to it using Eq. (3.3) where,

$$\alpha_{dB}L = 16.0 \text{ dB}$$

hence,

$$\alpha_{dB} = \frac{16.0}{8}$$

$$= 2.0 \text{ dB km}^{-1}$$

(c) As $\alpha_{dB} = 2\ dB\,km^{-1}$, the loss incurred along 10 km of the fiber is given by

$$\alpha_{dB}L = 2 \times 10 = 20 \text{ dB}$$

However, the link also has nine splices (at 1 km intervals) each with an attenuation of 1 dB. Therefore, the loss due to the splices is 9 dB.

Hence, the overall signal attenuation for the link is:

$$\textit{Signal attenuation} = 20 + 9 = 29 \text{ dB}$$

(d) To obtain a numerical value for the input/output power ratio, Eq. (3.2) may be used where:

$$\frac{P_i}{P_o} = 10^{29/10} = 794.3$$

A number of mechanisms are responsible for the signal attenuation within optical fibers. These mechanisms are influenced by the material composition, the preparation and purification technique, and the waveguide structure. They may be categorized within several major areas which include material absorption, material scattering (linear and nonlinear scattering), curve and microbending losses, mode coupling radiation losses and losses due to leaky modes. There are also losses at connectors and splices, as illustrated in Example 3.1. However, in this chapter we are interested solely in the characteristics of the fiber; connector and splice losses are dealt with in Section 5.2. It is instructive to consider in some detail the loss mechanisms within optical fibers in order to obtain an understanding of the problems associated with the design and fabrication of low loss waveguides.

3.3 Material absorption losses in silica glass fibers

Material absorption is a loss mechanism related to the material composition and the fabrication process for the fiber, which results in the dissipation of some of the transmitted optical power as heat in the waveguide. The absorption of the light may be intrinsic (caused by the interaction with one or more of the major components of the glass) or extrinsic (caused by impurities within the glass).

3.3.1 Intrinsic absorption

An absolutely pure silicate glass has little intrinsic absorption due to its basic material structure in the near-infrared region. However, it does have two major intrinsic absorption mechanisms at optical wavelengths which leave a low intrinsic absorption window over the 0.8 to 1.7 μm wavelength range, as illustrated in Figure 3.1, which shows a possible optical attenuation against wavelength characteristic for absolutely pure glass [Ref. 3]. It may be observed that there is a fundamental absorption edge, the peaks of which are centred in the ultraviolet wavelength region. This is due to the stimulation of electron transitions within the glass by higher energy excitations. The tail of this peak may extend into the window region at the shorter wavelengths, as illustrated in Figure 3.1. Also in the infrared

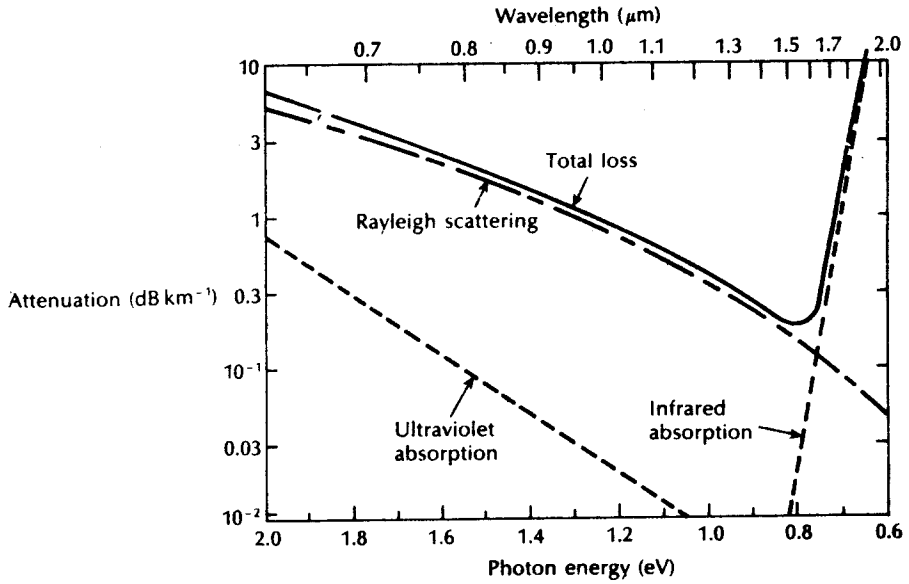

Figure 3.1 The attenuation spectra for the intrinsic loss mechanisms in pure GeO_2—SiO_2 glass [Ref. 3].

and far-infrared, normally at wavelengths above 7 μm, fundamentals of absorption bands from the interaction of photons with molecular vibrations within the glass occur. These give absorption peaks which again extend into the window region. The strong absorption bands occur due to oscillations of structural units such as Si—O (9.2 μm), P—O (8.1 μm), B—O (7.2 μm) and Ge—O (11.0 μm) within the glass. Hence, above 1.5 μm the tails of these largely far-infrared absorption peaks tend to cause most of the pure glass losses.

However, the effects of both these processes may be minimized by suitable choice of both core and cladding compositions. For instance, in some nonoxide glasses such as fluorides and chlorides, the infrared absorption peaks occur at much longer wavelengths which are well into the far-infrared (up to 50 μm), giving less attenuation to longer wavelength transmission compared with oxide glasses.

3.3.2 Extrinsic absorption

In practical optical fibers prepared by conventional melting techniques (see Section 4.3), a major source of signal attenuation is extrinsic absorption from transition metal element impurities. Some of the more common metallic impurities found in glasses are shown in the Table 3.1, together with the absorption losses caused by one part in 10^9 [Ref. 4]. It may be noted that certain of these impurities, namely chromium and copper, in their worst valence state can cause attenuation in excess of 1 dB km^{-1} in the near-infrared region. Transition element contamination may be

Table 3.1 Absorption losses caused by some of the more common metallic ion impurities in glasses, together with the absorption peak wavelength

	Peak wavelength (nm)	One part in 10^9 (dB km^{-1})
Cr^{3+}	625	1.6
C^{2+}	685	0.1
Cu^{2+}	850	1.1
Fe^{2+}	1100	0.68
Fe^{3+}	400	0.15
Ni^{2+}	650	0.1
Mn^{3+}	460	0.2
V^{4+}	725	2.7

reduced to acceptable levels (i.e. one part in 10^{10}) by glass refining techniques such as vapour-phase oxidation [Ref. 5] (see Section 4.4), which largely eliminates the effects of these metallic impurities.

However, another major extrinsic loss mechanism is caused by absorption due to water (as the hydroxyl or OH ion) dissolved in the glass. These hydroxyl groups are bonded into the glass structure and have fundamental stretching vibrations which occur at wavelengths between 2.7 and 4.2 μm depending on group position in the glass network. The fundamental vibrations give rise to overtones appearing almost harmonically at 1.38, 0.95 and 0.72 μm, as illustrated in Figure 3.2 [Ref. 6]. This

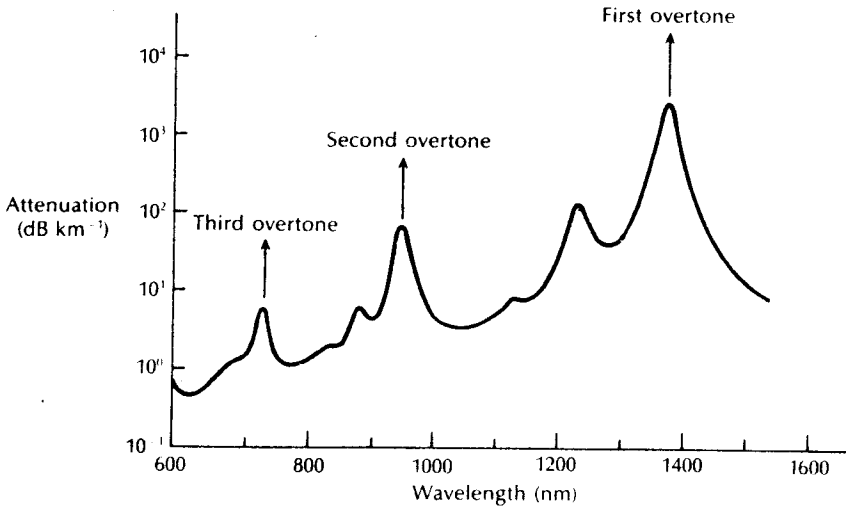

Figure 3.2 The absorption spectrum for the hydroxyl (OH) group in silica. Reproduced with permission from D. B. Keck, R. D. Maurer and P. C. Schultz, *Appl. Phys. Lett.*, **22**, p. 307, 1973.

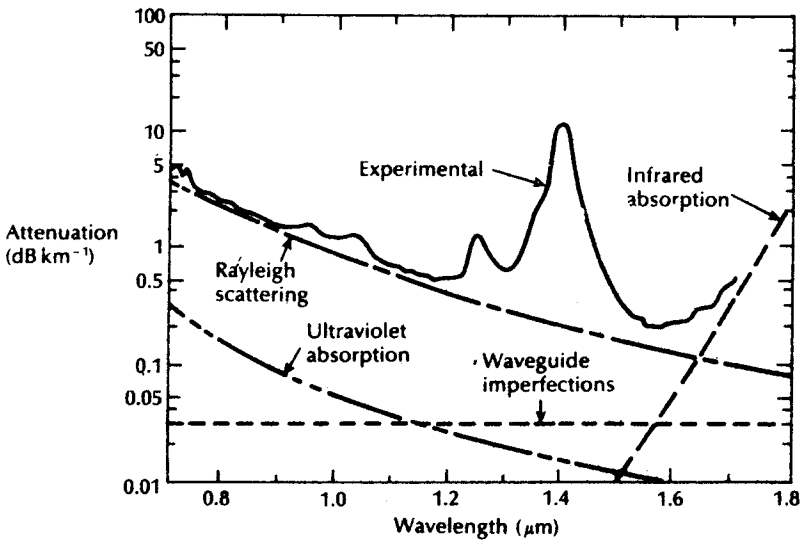

Figure 3.3 The measured attenuation spectrum for an ultra-low-loss single-mode fiber (solid line) with the calculated attenuation spectra for some of the loss mechanisms contributing to the overall fiber attenuation (dashed and dotted lines) [Ref. 3].

shows the absorption spectrum for the hydroxyl group in silica. Furthermore, combinations between the overtones and the fundamental SiO_2 vibration occur at 1.24, 1.13 and 0.88 μm, completing the absorption spectrum shown in Figure 3.2.

It may also be observed in Figure 3.2 that the only significant absorption band in the region below a wavelength of 1 μm is the second overtone at 0.95 μm which causes attenuation of about 1 dB km^{-1} for one part per million (ppm) of hydroxyl. At longer wavelengths the first overtone at 1.38 μm and its sideband at 1.24 μm are strong absorbers giving attenuation of about 2 dB km^{-1} ppm and 4 dB km^{-1} ppm respectively. Since most resonances are sharply peaked, narrow windows exist in the longer wavelength region around 1.3 and 1.55 μm which are essentially unaffected by OH absorption once the impurity level has been reduced below one part in 10^7. This situation is illustrated in Figure 3.3, which shows the attenuation spectrum of an ultra-low-loss single-mode fiber [Ref. 3]. It may be observed that the lowest attenuation for this fiber occurs at a wavelength of 1.55 μm and is 0.2 dB km^{-1}. This is approaching the minimum possible attenuation of around 0.18 dB km^{-1} at this wavelength [Ref. 8].

3.4 Linear scattering losses

Linear scattering mechanisms cause the transfer of some or all of the optical power contained within one propagating mode to be transferred linearly (proportionally

to the mode power) into a different mode. This process tends to result in attenuation of the transmitted light as the transfer may be to a leaky or radiation mode which does not continue to propagate within the fiber core, but is radiated from the fiber. It must be noted that as with all linear processes there is no change of frequency on scattering.

Linear scattering may be categorized into two major types: Rayleigh and Mie scattering. Both result from the nonideal physical properties of the manufactured fiber which are difficult and, in certain cases, impossible to eradicate at present.

3.4.1 Rayleigh scattering

Rayleigh scattering is the dominant intrinsic loss mechanism in the low absorption window between the ultraviolet and infrared absorption tails. It results from inhomogeneities of a random nature occurring on a small scale compared with the wavelength of the light. These inhomogeneities manifest themselves as refractive index fluctuations and arise from density and compositional variations which are frozen into the glass lattice on cooling. The compositional variations may be reduced by improved fabrication, but the index fluctuations caused by the freezing-in of density inhomogeneities are fundamental and cannot be avoided. The subsequent scattering due to the density fluctuations, which is in almost all directions, produces an attenuation proportional to $1/\lambda^4$ following the Rayleigh scattering formula [Ref. 9]. For a single component glass this is given by:

$$\gamma_R = \frac{8\pi^3}{3\lambda^4} n^8 p^2 \beta_c K T_F \tag{3.4}$$

where γ_R is the Rayleigh scattering coefficient, λ is the optical wavelength, n is the refractive index of the medium, p is the average photoelastic coefficient, β_c is the isothermal compressibility at a fictive temperature T_F, and K is Boltzmann's constant. The fictive temperature is defined as the temperature at which the glass can reach a state of thermal equilibrium and is closely related to the anneal temperature. Furthermore, the Rayleigh scattering coefficient is related to the transmission loss factor (transmissivity) of the fiber $\mathscr{T}$ following the relation [Ref. 10]:

$$\mathscr{T} = \exp(-\gamma_R L) \tag{3.5}$$

where L is the length of the fiber. It is apparent from Eq. (3.4) that the fundamental component of Rayleigh scattering is strongly reduced by operating at the longest possible wavelength. This point is illustrated in Example 3.2.

Example 3.2

Silica has an estimated fictive temperature of 1400 K with an isothermal compressibility of 7×10^{-11} m^{2}N^{-1} [Ref. 11]. The refractive index and the

photoelastic coefficient for silica are 1.46 and 0.286 respectively [Ref. 11]. Determine the theoretical attenuation in decibels per kilometre due to the fundamental Rayleigh scattering in silica at optical wavelengths of 0.63, 1.00 and 1.30 μm. Boltzmann's constant is 1.381×10^{-23} J K^{-1}.

Solution: The Rayleigh scattering coefficient may be obtained from Eq. (3.4) for each wavelength. However, the only variable in each case is the wavelength, and therefore the constant of proportionality of Eq. (3.4) applies in all cases. Hence:

$$\gamma_R = \frac{8\pi^3 n^8 p^2 \beta_c K T_f}{3\lambda^4}$$

$$= \frac{248.15 \times 20.65 \times 0.082 \times 7 \times 10^{-11} \times 1.381 \times 10^{-23} \times 1400}{3 \times \lambda^4}$$

$$= \frac{1.895 \times 10^{-28}}{\lambda^4} \text{ m}^{-1}$$

At a wavelength of 0.63 μm:

$$\gamma_R = \frac{1.895 \times 10^{-28}}{0.158 \times 10^{-24}} = 1.199 \times 10^{-3} \text{ m}^{-1}$$

The transmission loss factor for one kilometre of fiber may be obtained using Eq. (3.5),

$$\mathscr{T}_{km} = \exp(-\gamma_R L) = \exp(-1.199 \times 10^{-3} \times 10^3)$$
$$= 0.301$$

The attenuation due to Rayleigh scattering in dB km^{-1} may be obtained from Eq. (3.1) where:

$$\textit{Attenuation} = 10 \log_{10}(1/\mathscr{T}_{km}) = 10 \log_{10} 3.322$$
$$= 5.2 \text{ dB km}^{-1}$$

At a wavelength of 1.00 μm:

$$\gamma_R = \frac{1.895 \times 10^{-28}}{10^{-24}} = 1.895 \times 10^{-4} \text{ m}^{-1}$$

Using Eq. (3.5):

$$\mathscr{T}_{km} = \exp(-1.895 \times 10^{-4} \times 10^3) = \exp(-0.1895)$$
$$= 0.827$$

and Eq. (3.1):

$$\textit{Attenuation} = 10 \log_{10} 1.209 = 0.8 \text{ dB km}^{-1}$$

At a wavelength of 1.30 μm:

$$\gamma_R = \frac{1.895 \times 10^{-28}}{2.856 \times 10^{-24}} = 0.664 \times 10^{-4}$$

Using Eq. (3.5):

$$\mathscr{L}_{km} = \exp(-0.664 \times 10^{-4} \times 10^{3}) = 0.936$$

and Eq. (3.1):

$$Attenuation = 10 \log_{10} 1.069 = 0.3 \text{ dB km}^{-1}$$

The theoretical attenuation due to Rayleigh scattering in silica at wavelengths of 0.63, 1.00 and 1.30 μm, from Example 3.2, is 5.2, 0.8 and 0.3 dB km^{-1} respectively. These theoretical results are in reasonable agreement with experimental work. For instance, a low reported value for Rayleigh scattering in silica at a wavelength of 0.6328 μm is 3.9 dB km^{-1} [Ref. 11]. However, values of 4.8 dB km^{-1} [Ref. 12] and 5.4 dB km^{-1} [Ref. 13] have also been reported. The predicted attenuation due to Rayleigh scattering against wavelength is indicated by a broken line on the attenuation characteristics shown in Figures 3.1 and 3.3.

3.4.2 Mie scattering

Linear scattering may also occur at inhomogeneities which are comparable in size to the guided wavelength. These result from the nonperfect cylindrical structure of the waveguide and may be caused by fiber imperfections such as irregularities in the core–cladding interface, core–cladding refractive index differences along the fiber length, diameter fluctuations, strains and bubbles. When the scattering inhomogeneity size is greater than $\lambda/10$, the scattered intensity which has an angular dependence can be very large.

The scattering created by such inhomogeneities is mainly in the forward direction and is called Mie scattering. Depending upon the fiber material, design and manufacture, Mie scattering can cause significant losses. The inhomogeneities may be reduced by:

(a) removing imperfections due to the glass manufacturing process;
(b) carefully controlled extrusion and coating of the fiber;
(c) increasing the fiber guidance by increasing the relative refractive index difference.

By these means it is possible to reduce Mie scattering to insignificant levels.

3.5 Nonlinear scattering losses

Optical waveguides do not always behave as completely linear channels whose increase in output optical power is directly proportional to the input optical power. Several nonlinear effects occur, which in the case of scattering cause disproportionate attenuation, usually at high optical power levels. This nonlinear scattering

causes the optical power from one mode to be transferred in either the forward or backward direction to the same, or other modes, at a different frequency. It depends critically upon the optical power density within the fiber and hence only becomes significant above threshold power levels.

The most important types of nonlinear scattering within optical fibers are stimulated Brillouin and Raman scattering, both of which are usually only observed at high optical power densities in long single-mode fibers. These scattering mechanisms in fact give optical gain but with a shift in frequency, thus contributing to attenuation for light transmission at a specific wavelength. However, it may be noted that such nonlinear phenomena can also be used to give optical amplification in the context of integrated optical techniques (see Section 10.8). In addition, these nonlinear processes are explored in further detail both following and in Section 3.14.

3.5.1 Stimulated Brillouin scattering

Stimulated Brillouin scattering (SBS) may be regarded as the modulation of light through thermal molecular vibrations within the fiber. The scattered light appears as upper and lower sidebands which are separated from the incident light by the modulation frequency. The incident photon in this scattering process produces a phonon* of acoustic frequency as well as a scattered photon. This produces an optical frequency shift which varies with the scattering angle because the frequency of the sound wave varies with acoustic wavelength. The frequency shift is a maximum in the backward direction reducing to zero in the forward direction making SBS a mainly backward process.

As indicated previously, Brillouin scattering is only significant above a threshold power density. Assuming that the polarization state of the transmitted light is not maintained (see Section 3.12), it may be shown [Ref 16] that the threshold power P_B is given by:

$$P_B = 4.4 \times 10^{-3} d^2 \lambda^2 \alpha_{dB} \nu \text{ watts} \tag{3.6}$$

where d and λ are the fiber core diameter and the operating wavelength, respectively, both measured in micrometres, α_{dB} is the fiber attenuation in decibels per kilometre and ν is the source bandwidth (i.e. injection laser) in gigahertz. The expression given in Eq. (3.6) allows the determination of the threshold optical power which must be launched into a single-mode optical fiber before SBS occurs (see Example 3.3).

3.5.2 Stimulated Raman scattering

Stimulated Raman scattering (SRS) is similar to stimulated Brillouin scattering except that a high frequency optical phonon rather than an acoustic phonon is

* The phonon is a quantum of an elastic wave in a crystal lattice. When the elastic wave has a frequency f, the quantized unit of the phonon has energy hf joules, where h is Planck's constant.

generated in the scattering process. Also, SRS can occur in both the forward and backward directions in an optical fiber, and may have an optical power threshold of up to three orders of magnitude higher than the Brillouin threshold in a particular fiber.

Using the same criteria as those specified for the Brillouin scattering threshold given in Eq. (3.6), it may be shown [Ref. 16] that the threshold optical power for SRS P_R in a long single-mode fiber is given by:

$$P_R = 5.9 \times 10^{-2} d^2 \lambda \alpha_{dB} \text{ watts} \tag{3.7}$$

where d, λ and α_{dB} are as specified for Eq. (3.6).

Example 3.3

A long single-mode optical fiber has an attenuation of 0.5 dB km^{-1} when operating at a wavelength of 1.3 μm. The fiber core diameter is 6 μm and the laser source bandwidth is 600 MHz. Compare the threshold optical powers for stimulated Brillouin and Raman scattering within the fiber at the wavelength specified.

Solution: The threshold optical power for SBS is given by Eq. (3.6) as

$$\begin{aligned} P_B &= 4.4 \times 10^{-3} d^2 \lambda^2 \alpha_{dB} \nu \\ &= 4.4 \times 10^{-3} \times 6^2 \times 1.3^2 \times 0.5 \times 0.6 \\ &= 80.3 \text{ mW} \end{aligned}$$

The threshold optical power for SRS may be obtained from Eq. (3.7), where:

$$\begin{aligned} P_R &= 5.9 \times 10^{-2} d^2 \lambda \alpha_{dB} \\ &= 5.9 \times 10^{-2} \times 6^2 \times 1.3 \times 0.5 \\ &= 1.38 \text{ W} \end{aligned}$$

In Example 3.3, the Brillouin threshold occurs at an optical power level of around 80 mW whilst the Raman threshold is approximately seventeen times larger. It is therefore apparent that the losses introduced by nonlinear scattering may be avoided by use of a suitable optical signal level (i.e. working below the threshold optical powers). However, it must be noted that the Brillouin threshold has been reported [Ref. 17] as occurring at optical powers as low as 10 mW in single-mode fibers. Nevertheless, this is still a high power level for optical communications and may be easily avoided. SBS and SRS are not usually observed in multimode fibers because their relatively large core diameters make the threshold optical power levels extremely high. Moreover, it should be noted that the threshold optical powers for both these scattering mechanisms may be increased by suitable adjustment of the other parameters in Eqs. (3.6) and (3.7). In this context, operation at the longest possible wavelength is advantageous although this may be offset by the reduced fiber attenuation (from Rayleigh scattering and material absorption) normally obtained.

3.6 Fiber bend loss

Optical fibers suffer radiation losses at bends or curves on their paths. This is due to the energy in the evanescent field at the bend exceeding the velocity of light in the cladding and hence the guidance mechanism is inhibited, which causes light energy to be radiated from the fiber. An illustration of this situation is shown in Figure 3.4. The part of the mode which is on the outside of the bend is required to travel faster than that on the inside so that a wavefront perpendicular to the direction of propagation is maintained. Hence, part of the mode in the cladding needs to travel faster than the velocity of light in that medium. As this is not possible, the energy associated with this part of the mode is lost through radiation. The loss can generally be represented by a radiation attenuation coefficient which has the form [Ref. 19]:

$$\alpha_r = c_1 \exp(-c_2 R)$$

where R is the radius of curvature of the fiber bend and c_1, c_2 are constants which are independent of R. Furthermore, large bending losses tend to occur in multimode fibers at a critical radius of curvature R_c which may be estimated from [Ref. 20]:

$$R_c \simeq \frac{3n_1^2\lambda}{4\pi(n_1^2 - n_2^2)^{\frac{3}{2}}} \tag{3.8}$$

It may be observed from the expression given in Eq. (3.8) that potential macrobending losses may be reduced by:

(a) designing fibers with large relative refractive index differences;
(b) operating at the shortest wavelength possible.

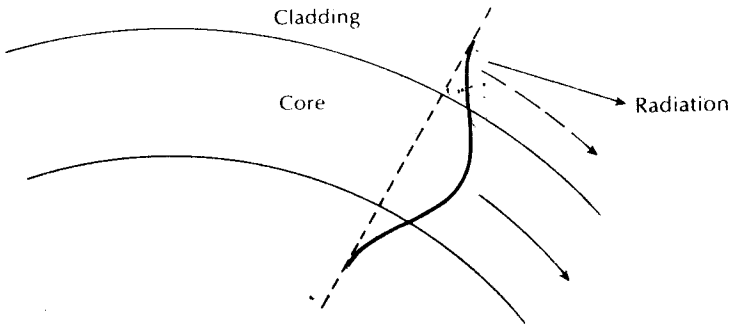

Figure 3.4 An illustration of the radiation loss at a fiber bend. The part of the mode in the cladding outside the dashed arrowed line may be required to travel faster than the velocity of light in order to maintain a plane wavefront. Since it cannot do this, the energy contained in this part of the mode is radiated away.

The above criteria for the reduction of bend losses also apply to single-mode fibers. One theory [Ref. 21], based on the concept of a single quasi-guided mode, provides an expression from which the critical radius of curvature for a single-mode fiber R_{cs} can be estimated as:

$$R_{cs} \simeq \frac{20\lambda}{(n_1 - n_2)^{\frac{3}{2}}} \left(2.748 - 0.996 \frac{\lambda}{\lambda_c}\right)^{-3} \tag{3.9}$$

where λ_c is the cutoff wavelength for the single-mode fiber. Hence again, for a specific single-mode fiber (that is, a fixed relative index difference and cutoff wavelength), the critical wavelength of the radiated light becomes progressively shorter as the bend radius is decreased. The effect of this factor and that of the relative refractive index difference on the critical bending radius is demonstrated in the following example.

Example 3.4

Two step index fibers exhibit the following parameters:

(a) A multimode fiber with a core refractive index of 1.500, a relative refractive index difference of 3% and an operating wavelength of 0.82 μm.
(b) An 8 μm core diameter single-mode fiber with a core refractive index the same as (a), a relative refractive index difference of 0.3% and an operating wavelength of 1.55 μm.

Estimate the critical radius of curvature at which large bending losses occur in both cases.

Solution: (a) The relative refractive index difference is given by Eq. (2.9) as:

$$\Delta = \frac{n_1^2 - n_2^2}{2n_1^2}$$

Hence

$$n_2^2 = n_1^2 - 2\Delta n_1^2 = 2.250 - 0.06 \times 2.250$$
$$= 2.115$$

Using Eq. (3.8) for the multimode fiber critical radius of curvature:

$$R_c \simeq \frac{3n_1^2\lambda}{4\pi(n_1^2 - n_2^2)^{\frac{3}{2}}} = \frac{3 \times 2.250 \times 0.82 \times 10^{-6}}{4\pi \times (0.135)^{\frac{3}{2}}}$$
$$= 9\ \mu\text{m}$$

(b) Again, from Eq. (2.9):

$$n_2^2 = n_1^2 - 2\Delta n_1^2 = 2.250 - (0.006 \times 2.250)$$
$$= 2.237$$

The cutoff wavelength for the single-mode fiber is given by Eq. (2.98) as:

$$\lambda_c = \frac{2\pi a n_1 (2\Delta)^{\frac{1}{2}}}{2.405}$$

$$= \frac{2\pi \times 4 \times 10^{-6} \times 1.500\ (0.06)^{\frac{1}{2}}}{2.405}$$

$$= 1.214\ \mu\text{m}$$

Substituting into Eq. (3.9) for the critical radius of curvature for the single-mode fiber gives:

$$R_{cs} \simeq \frac{20 \times 1.55 \times 10^{-6}}{(0.043)^{\frac{1}{2}}} \left(2.748 - \frac{0.996 \times 1.55 \times 10^{-6}}{1.214 \times 10^{-6}}\right)^{-3}$$

$$= 34\ \text{mm}$$

Example 3.4 shows that the critical radius of curvature for guided modes can be made extremely small (e.g. 9 μm), although this may be in conflict with the preferred design and operational characteristics. Nevertheless, for most practical purposes, the critical radius of curvature is relatively small (even when considering the case of a long wavelength single-mode fiber, it was found to be around 34 mm) to avoid severe attenuation of the guided mode(s) at fiber bends. However, modes propagating close to cutoff, which are no longer fully guided within the fiber core, may radiate at substantially larger radii of curvature. Thus it is essential that sharp bends, with a radius of curvature approaching the critical radius, are avoided when optical fiber cables are installed. Finally, it is important that microscopic bends with radii of curvature approximating to the fiber radius are not produced in the fiber cabling process. These so-called microbends, which can cause significant losses from cabled fiber, are discussed further in Section 4.8.1.

3.7 Mid-infrared and far-infrared transmission

In the near-infrared region of the optical spectrum, fundamental silica fiber attenuation is dominated by Rayleigh scattering and multiphonon absorption from the infrared absorption edge (See Figure 3.2). Therefore, the total loss decreases as the operational transmission wavelength increases until a crossover point is reached around a wavelength of 1.55 μm where the total fiber loss again increases because at longer wavelengths the loss is dominated by the phonon absorption edge. Since the near fundamental attenuation limits for near-infrared silicate glass fibers have been achieved, more recently researchers have turned their attention to the mid-infrared (2 to 5 μm) and the far-infrared (8 to 12 μm) optical wavelengths.

In order to obtain lower loss fibers it is necessary to produce glasses exhibiting longer infrared cutoff wavelengths. Potentially, much lower losses can be achieved if the transmission window of the material can be extended further into the infrared by utilizing constituent atoms of higher atomic mass and if it can be drawn into fiber exhibiting suitable strength and chemical durability. The reason for this possible loss reduction is due to Rayleigh scattering which displays a λ^{-4} dependence and hence becomes much reduced as the wavelength is increased. For example, the scattering loss is reduced by a factor of 16 when the optical wavelength is doubled. Thus it may be possible to obtain losses of the order of 0.01 dB km^{-1} at a wavelength of 2.55 μm, with even lower losses at wavelengths of between 3 μm and 5 μm [Ref. 23].

Candidate glass forming systems for mid-infrared transmission are fluoride, fluoride–chloride, chalcogenide and possibly oxide. In particular, heavy metal oxide glasses based on bismuth and gallium oxides offer a near equivalent transmittance range to many of the fluoride glasses and hence show promise if their scatter losses can be made acceptably low [Ref. 24]. Chalcogenide glasses, which generally comprise one or more of the elements S, Se and Te, together with one or more elements Ge, Si, As and Sb, are capable of optical transmission in both the mid-infrared and far-infrared regions.* However, research activities into far-infrared transmission using chalcogenide glasses, halide glasses and halide crystal fibers are at present mainly concerned with radiometry, infrared imaging and power transmission rather than telecommunications [Ref. 25].

The research activities into ultra-low-loss fibers for long-haul repeaterless communications have to date centred on the fluorozirconates, with zirconium fluoride (ZrF_4) as the major constituent and fluorides of barium, lanthanum, aluminium, gadolinium, sodium, lithium and occasionally lead added as modifiers and stabilizers [Ref. 26]. Such alkali additives improve the glass stability and working characteristics. Moreover, hafnium tetrafluoride (HfF_4) can be substituted for ZrF_4 to vary the refractive index and form fluorohafnate glasses. Both these glass systems offer transmittance to a wavelength of around 5.5 μm [Ref. 23].

Extensive work has been undertaken on two particular heavy metal fluoride systems, namely: zirconium–barium–lanthanum–aluminium fluoride (ZBLA) and zirconium–barium–gadolinium–aluminium fluoride (ZBGA). Furthermore, sodium fluoride is often added to ZBLA to increase its stability and form ZBLAN glass. In this case the core–cladding refractive index differences are obtained by varying the sodium fluoride level or by partially substituting hafnium tetrafluoride for the zirconium, whereas with ZBGA the aluminium fluoride content is usually varied. Typically, the above glasses contain approximately 50 to 60% ZrF_4 or HfF_4, together with 30 to 40% BaF_2, with the other alkali and rare earth fluorides completing the composition.

In order to fabricate low loss, long length fluoride fibers a basic problem concerned with reducing the extrinsic losses remains to be resolved [Ref. 27]. At

* A typical chalcogenide fiber glass is As_2S_3.

present the most critical and difficult problems are associated with the minimization of the scattering losses resulting from extrinsic factors such as defects, waveguide imperfections and radiation caused by mechanical deformation. The estimated losses of around 0.01 dB km^{-1} at a wavelength of 2.5 μm for ZrF_4-based fibers are derived from an assessment of the extrinsic losses due to ultraviolet and infrared absorptions together with Rayleigh scattering. However, experimental losses obtained so far remain significantly higher (i.e. one order of magnitude) than this estimated value. Nevertheless, it is useful to consider the theoretical characteristics for intrinsic losses obtained for a range of materials which are displayed in Figure 3.5 [Ref. 28]. The effect of increasing the atomic weight of the anion from oxide to fluoride may be clearly observed. Although the theoretical losses shown in Figure 3.5 cannot yet be achieved in practical fiber, progress has been made in relation to the fabrication of heavy metal fluoride glass fibers, particularly for single-mode operation [Ref. 29].

Materials such as $ZnCl_2$ and As_2S_3 are also being considered for mid-infrared transmission since this is their region of minimum loss, as can be observed in

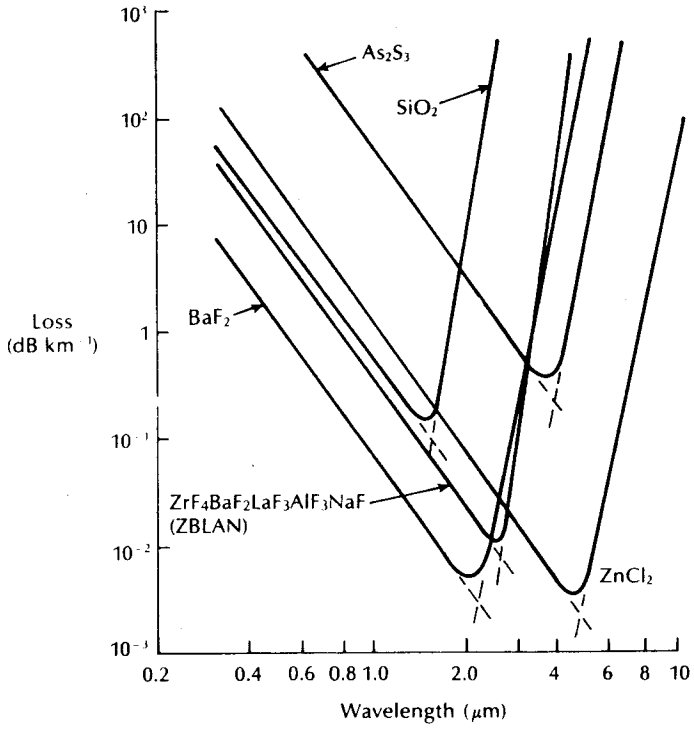

Figure 3.5 Theoretical intrinsic losses for a number of mid-infrared transmitting materials. Reproduced with permission from J. A. Savage, 'Materials for infrared fiber optics', Mat. Sci. Rep., **2**, pp. 99–138, 1987.

Figure 3.5. In addition these glasses offer potential for far-infrared transmission applications as fiber lengths of a few metres may prove sufficient for use with CO_2 laser radiation.* Moreover, both monocrystalline and polycrystalline halide fibers [Ref. 23] as well as hollow core glass fibers [Ref. 30] are being studied to assess their potential for high power transmission applications. A commercial example in the former case is Kristen 5 (KRS-5) fiber fabricated from TlBr and TlI produced by Horiba of Japan [Ref. 25].

3.8 Dispersion

Dispersion of the transmitted optical signal causes distortion for both digital and analog transmission along optical fibers. When considering the major implementation of optical fiber transmission which involves some form of digital modulation, then dispersion mechanisms within the fiber cause broadening of the transmitted light pulses as they travel along the channel. The phenomenon is illustrated in Figure 3.6, where it may be observed that each pulse broadens and overlaps with its neighbours, eventually becoming indistinguishable at the receiver input. The effect is known as intersymbol interference (ISI). Thus an increasing number of errors may be encountered on the digital optical channel as the ISI becomes more pronounced. The error rate is also a function of the signal attenuation on the link and the subsequent signal to noise ratio (SNR) at the receiver. This factor is not pursued further here but is considered in detail in Section 11.6.3. However, signal dispersion alone limits the maximum possible bandwidth attainable with a particular optical fiber to the point where individual symbols can no longer be distinguished.

For no overlapping of light pulses down on an optical fiber link the digital bit rate B_T must be less than the reciprocal of the broadened (through dispersion) pulse duration (2τ). Hence:

$$B_T \leqslant \frac{1}{2\tau} \tag{3.10}$$

This assumes that the pulse broadening due to dispersion on the channel is τ which dictates the input pulse duration which is also τ. Hence Eq. (3.10) gives a conservative estimate of the maximum bit rate that may be obtained on an optical fiber link as $1/2\tau$.

Another more accurate estimate of the maximum bit rate for an optical channel with dispersion may be obtained by considering the light pulses at the output to have a Gaussian shape with an rms width of σ. Unlike the relationship given in Eq. (3.10), this analysis allows for the existence of a certain amount of signal overlap on the channel, whilst avoiding any SNR penalty which occurs when intersymbol interference becomes pronounced. The maximum bit rate is given approximately by

* Operating at a wavelength of 10.6 μm.

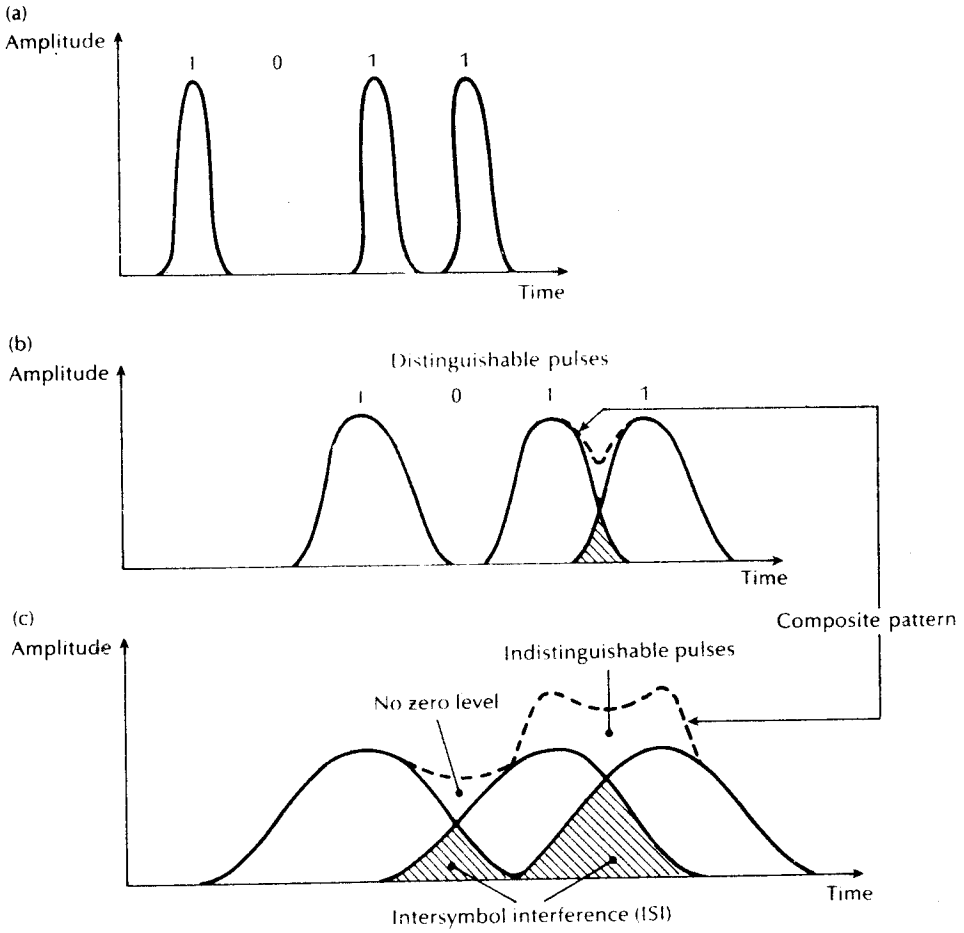

Figure 3.6 An illustration using the digital bit pattern 1011 of the broadening of light pulses as they are transmitted along a fiber: (a) fiber input; (b) fiber output at a distance L_1; (c) fiber output at a distance $L_2 > L_1$.

(see Appendix B):

$$B_T(\max) \simeq \frac{0.2}{\sigma} \text{ bit s}^{-1} \tag{3.11}$$

It must be noted that certain sources [Refs. 31, 32] give the constant term in the numerator of Eq. (3.11) as 0.25. However, we take the slightly more conservative estimate given, following Olshansky [Ref. 9] and Gambling *et al.* [Ref. 33]. Equation (3.11) gives a reasonably good approximation for other pulse shapes which may occur on the channel resulting from the various dispersive mechanisms

within the fiber. Also, σ may be assumed to represent the rms impulse response for the channel, as discussed further in Section 3.10.1.

The conversion of bit rate to bandwidth in hertz depends on the digital coding format used. For metallic conductors when a nonreturn to zero code is employed, the binary one level is held for the whole bit period τ. In this case there are two bit periods in one wavelength (i.e. two bits per second per hertz), as illustrated in Figure 3.7(a). Hence the maximum bandwidth B is one half the maximum data rate or

$$B_T(\max) = 2B \tag{3.12}$$

However, when a return code is considered, as shown in Figure 3.7(b), the binary one level is held for only part (usually half) the bit period. For this signalling scheme the data rate is equal to the bandwidth in hertz (i.e. one bit per second per hertz) and thus $B_T = B$. The bandwidth B for metallic conductors is also usually defined by the electrical 3 dB points (i.e. the frequencies at which the electrical power has dropped to one half of its constant maximum value). However, when the 3 dB optical bandwidth of a fiber is considered it is significantly larger than the corresponding 3 dB electrical bandwidth for the reasons discussed in Section 7.4.3. Hence, when the limitations in the bandwidth of a fiber due to dispersion are stated (i.e. optical bandwidth B_{opt}), it is usually with regard to a return to zero code where the bandwidth in hertz is considered equal to the digital bit rate. Within the context of dispersion the bandwidths expressed in this chapter will follow this general criterion unless otherwise stated. However, as is made clear in Section 7.4.3, when electro-optical devices and optical fiber systems are considered it is more usual to state the electrical 3 dB bandwidth, this being the more useful measurement when

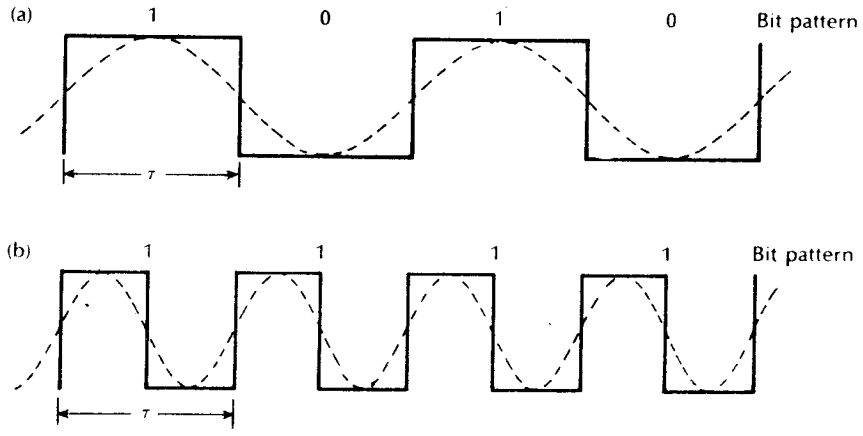

Figure 3.7 Schematic illustration of the relationships of the bit rate to wavelength for digital codes: (a) nonreturn to zero (NRZ); (b) return to zero (RZ).

interfacing an optical fiber link to electrical terminal equipment. Unfortunately, the terms of bandwidth measurement are not always made clear and the reader must be warned that this omission may lead to some confusion when specifying components and materials for optical fiber communication systems.

Figure 3.8 shows the three common optical fiber structures, multimode step index, multimode graded index and single-mode step index, whilst diagrammatically illustrating the respective pulse broadening associated with each fiber type. It may be observed that the multimode step index fiber exhibits the greatest dispersion of a transmitted light pulse and the multimode graded index fiber gives a considerably improved performance. Finally, the single-mode fiber gives the minimum pulse broadening and thus is capable of the greatest transmission bandwidths which are currently in the gigahertz range, whereas transmission via multimode step index fiber is usually limited to bandwidths of a few tens of megahertz. However, the amount of pulse broadening is dependent upon the distance the pulse travels within the fiber, and hence for a given optical fiber link

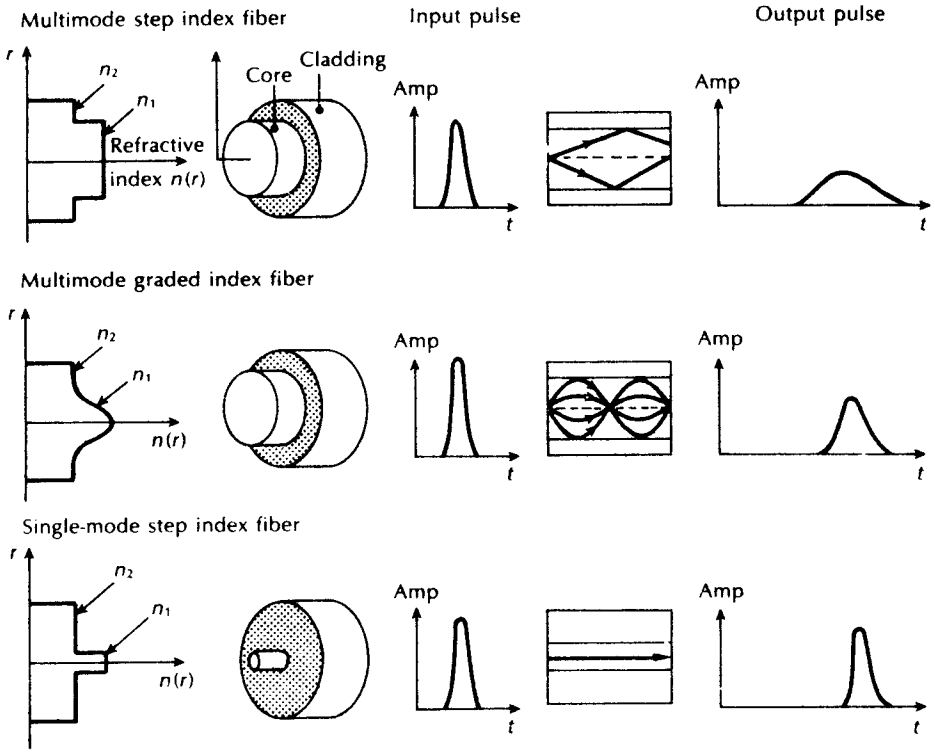

Figure 3.8 Schematic diagram showing a multimode step index fiber, multimode graded index fiber and single-mode step index fiber, and illustrating the pulse broadening due to intermodal dispersion in each fiber type.

the restriction on usable bandwidth is dictated by the distance between regenerative repeaters (i.e. the distance the light pulse travels before it is reconstituted). Thus the measurement of the dispersive properties of a particular fiber is usually stated as the pulse broadening in time over a unit length of the fiber (i.e. ps km^{-1}).

Hence, the number of optical signal pulses which may be transmitted in a given period, and therefore the information-carrying capacity of the fiber, is restricted by the amount of pulse dispersion per unit length. In the absence of mode coupling or filtering, the pulse broadening increases linearly with fiber length and thus the bandwidth is inversely proportional to distance. This leads to the adoption of a more useful parameter for the information-carrying capacity of an optical fiber which is known as the bandwidth–length product (i.e. $B_{opt} \times L$). The typical best bandwidth–length products for the three fibers shown in Figure 3.8, are 20 MHz km, 1 GHz km and 100 GHz km for multimode step index, multimode graded index and single-mode step index fibers respectively.

Example 3.5

A multimode graded index fiber exhibits total pulse broadening of 0.1 μs over a distance of 15 km. Estimate:

(a) the maximum possible bandwidth on the link assuming no intersymbol interference;
(b) the pulse dispersion per unit length;
(c) the bandwidth–length product for the fiber.

Solution: (a) The maximum possible optical bandwidth which is equivalent to the maximum possible bit rate (for return to zero pulses) assuming no ISI may be obtained from Eq. (3.10), where:

$$B_{opt} = B_T = \frac{1}{2\tau} = \frac{1}{0.2 \times 10^{-6}} = 5 \text{ MHz}$$

(b) The dispersion per unit length may be acquired simply by dividing the total dispersion by the total length of the fiber

$$\text{dispersion} = \frac{0.1 \times 10^{-6}}{15} = 6.67 \text{ ns km}^{-1}$$

(c) The bandwidth–length product may be obtained in two ways. Firstly by simply multiplying the maximum bandwidth for the fiber link by its length. Hence:

$$B_{opt} L = 5 \text{ MHz} \times 15 \text{ km} = 75 \text{ MHz km}$$

Alternatively, it may be obtained from the dispersion per unit length using Eq. (3.10) where:

$$B_{opt} L = \frac{1}{2 \times 6.67 \times 10^{-9}} = 75 \text{ MHz km}$$

In order to appreciate the reasons for the different amounts of pulse broadening within the various types of optical fiber, it is necessary to consider the dispersive mechanisms involved. These include material dispersion, waveguide dispersion, intermodal dispersion and profile dispersion which are considered in the following sections.

3.9 Intramodal dispersion

Intramodal or chromatic dispersion may occur in all types of optical fiber and results from the finite spectral linewidth of the optical source. Since optical sources do not emit just a single frequency but a band of frequencies (in the case of the injection laser corresponding to only a fraction of a per cent of the centre frequency, whereas for the LED it is likely to be a significant percentage), then there may be propagation delay differences between the different spectral components of the transmitted signal. This causes broadening of each transmitted mode and hence intramodal dispersion. The delay differences may be caused by the dispersive properties of the waveguide material (material dispersion) and also guidance effects within the fiber structure (waveguide dispersion).

3.9.1 Material dispersion

Pulse broadening due to material dispersion results from the different group velocities of the various spectral components launched into the fiber from the optical source. It occurs when the phase velocity of a plane wave propagating in the dielectric medium varies nonlinearly with wavelength, and a material is said to exhibit material dispersion when the second differential of the refractive index with respect to wavelength is not zero (i.e. $d^2n/d\lambda^2 \neq 0$). The pulse spread due to material dispersion may be obtained by considering the group delay τ_g in the optical fiber which is the reciprocal of the group velocity v_g defined by Eqs. (2.37) and (2.40). Hence the group delay is given by:

$$\tau_g = \frac{d\beta}{d\omega} = \frac{1}{c}\left(n_1 - \lambda \frac{dn_1}{d\lambda}\right) \tag{3.13}$$

where n_1 is the refractive index of the core material. The pulse delay τ_m due to material dispersion in a fiber of length L is therefore:

$$\tau_m = \frac{L}{c}\left(n_1 - \lambda \frac{dn_1}{d\lambda}\right) \tag{3.14}$$

For a source with rms spectral width σ_λ and a mean wavelength λ, the rms pulse broadening due to material dispersion σ_m may be obtained from the expansion of Eq. (3.14) in a Taylor series about λ where:

$$\sigma_m = \sigma_\lambda \frac{d\tau_m}{d\lambda} + \sigma_\lambda \frac{2d^2\tau_m}{d\lambda^2} + \cdots \tag{3.15}$$

As the first term in Eq. (3.15) usually dominates, especially for sources operating over the 0.8 to 0.9 μm wavelength range, then:

$$\sigma_m \simeq \sigma_\lambda \frac{d\tau_m}{d\lambda} \tag{3.16}$$

Hence the pulse spread may be evaluated by considering the dependence of τ_m on λ, where from Eq. (3.14):

$$\frac{d\tau_m}{d\lambda} = \frac{L\lambda}{c}\left[\frac{dn_1}{d\lambda} - \frac{d^2n_1}{d\lambda^2} - \frac{dn_1}{d\lambda}\right]$$

$$= \frac{-L\lambda}{c}\frac{d^2n_1}{d\lambda^2} \tag{3.17}$$

Therefore, substituting the expression obtained in Eq. (3.17) into Eq. (3.16), the rms pulse broadening due to material dispersion is given by:

$$\sigma_m \simeq \frac{\sigma_\lambda L}{c}\left|\lambda \frac{d^2n_1}{d\lambda^2}\right| \tag{3.18}$$

The material dispersion for optical fibers is sometimes quoted as a value for $|\lambda^2(d^2n_1/d\lambda^2)|$ or simply $|d^2n_1/d\lambda^2|$.

However, it may be given in terms of a material dispersion parameter M which is defined as:

$$M = \frac{1}{L}\frac{d\tau_m}{d\lambda} = \frac{\lambda}{c}\left|\frac{d^2n_1}{d\lambda^2}\right| \tag{3.19}$$

and which is often expressed in units of ps nm^{-1} km^{-1}.

Example 3.6

A glass fiber exhibits material dispersion given by $|\lambda^2(d^2n_1/d\lambda^2)|$ of 0.025. Determine the material dispersion parameter at a wavelength of 0.85 μm, and estimate the rms pulse broadening per kilometre for a good LED source with an rms spectral width of 20 nm at this wavelength.

Solution: The material dispersion parameter may be obtained from Eq. (3.19):

$$M = \frac{\lambda}{c}\left|\frac{d^2n_1}{d\lambda^2}\right| = \frac{1}{c\lambda}\left|\lambda^2\frac{d^2n_1}{d\lambda^2}\right|$$

$$= \frac{0.025}{2.998 \times 10^5 \times 850}\ \text{s nm}^{-1}\text{km}^{-1}$$

$$= 98.1\ \text{ps nm}^{-1}\text{km}^{-1}$$

The rms pulse broadening is given by Eq. (3.18) as:

$$\sigma_m \simeq \frac{\sigma_\lambda L}{c} \left| \lambda \frac{d^2 n_1}{d\lambda^2} \right|$$

Therefore in terms of the material dispersion parameter M defined by Eq. (3.19):

$$\sigma_m \simeq \sigma_\lambda L M$$

Hence, the rms pulse broadening per kilometre due to material dispersion:

$$\sigma_m(1 \text{ km}) = 20 \times 1 \times 98.1 \times 10^{-12} = 1.96 \text{ ns km}^{-1}$$

Figure 3.9 shows the variation of the material dispersion parameter M with wavelength for pure silica [Ref. 34]. It may be observed that the material dispersion tends to zero in the longer wavelength region around 1.3 μm (for pure silica). This provides an additional incentive (other than low attenuation) for operation at longer wavelengths where the material dispersion may be minimized. Also, the use of an injection laser with a narrow spectral width rather than an LED as the optical source leads to a substantial reduction in the pulse broadening due to material dispersion, even in the shorter wavelength region.

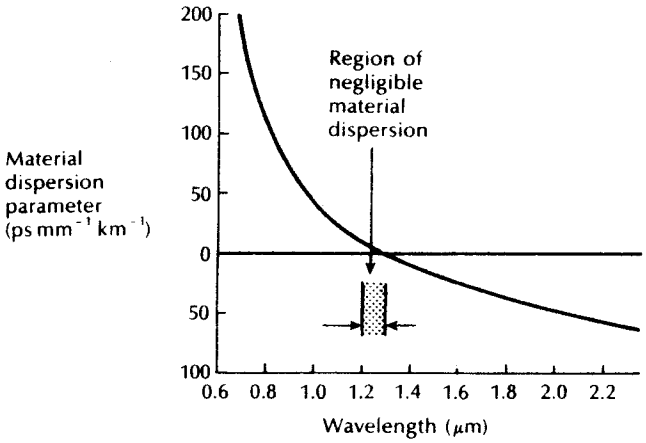

Figure 3.9 The material dispersion parameter for silica as a function of wavelength. Reproduced with permission from D. N. Payne and W. A. Gambling, *Electron. Lett.*, **11**, p. 176, 1975.

Example 3.7

Estimate the rms pulse broadening per kilometre for the fiber in Example 3.6 when the optical source used is an injection laser with a relative spectral width σ_λ/λ of 0.0012 at a wavelength of 0.85 μm.

Solution: The rms spectral width may be obtained from the relative spectral width by:

$$\sigma_\lambda = 0.0012\lambda = 0.0012 \times 0.85 \times 10^{-6}$$
$$= 1.02 \text{ nm}$$

The rms pulse broadening in terms of the material dispersion parameter following Example 3.6 is given by:

$$\sigma_m \simeq \sigma_\lambda LM$$

Therefore, the rms pulse broadening per kilometre due to material dispersion is:

$$\sigma_m \simeq 1.02 \times 1 \times 98.1 \times 10^{-12} = 0.10 \text{ ns km}^{-1}$$

Hence, in this example the rms pulse broadening is reduced by a factor of around 20 (i.e. equivalent to the reduced rms spectral width of the injection laser source) compared with that obtained with the LED source of Example 3.6.

3.9.2 Waveguide dispersion

The waveguiding of the fiber may also create intramodal dispersion. This results from the variation in group velocity with wavelength for a particular mode. Considering the ray theory approach it is equivalent to the angle between the ray and the fiber axis varying with wavelength which subsequently leads to a variation in the transmission times for the rays, and hence dispersion. For a single mode whose propagation constant is β, the fiber exhibits waveguide dispersion when $(d^2\beta)/(d\lambda^2) \neq 0$. Multimode fibers, where the majority of modes propagate far from cutoff, are almost free of waveguide dispersion and it is generally negligible compared with material dispersion (≈ 0.1 to 0.2 ns km^{-1}) [Ref. 34]. However, with single-mode fibers where the effects of the different dispersion mechanisms are not easy to separate, waveguide dispersion may be significant (see Section 3.11.2).

3.10 Intermodal dispersion

Pulse broadening due to intermodal dispersion (sometimes referred to simply as modal or mode dispersion) results from the propagation delay differences between modes within a multimode fiber. As the different modes which constitute a pulse in a multimode fiber travel along the channel at different group velocities, the pulse width at the output is dependent upon the transmission times of the slowest and fastest modes. This dispersion mechanism creates the fundamental difference in the overall dispersion for the three types of fiber shown in Figure 3.8. Thus multimode step index fibers exhibit a large amount of intermodal dispersion which gives the greatest pulse broadening. However, intermodal dispersion in multimode fibers may be reduced by adoption of an optimum refractive index profile which is provided

by the near parabolic profile of most graded index fibers. Hence, the overall pulse broadening in multimode graded index fibers is far less than that obtained in multimode step index fibers (typically by a factor of 100). Thus graded index fibers used with a multimode source give a tremendous bandwidth advantage over multimode step index fibers.

Under purely single-mode operation there is no intermodal dispersion and therefore pulse broadening is solely due to the intramodal dispersion mechanisms. In theory, this is the case with single-mode step index fibers where only a single mode is allowed to propagate. Hence they exhibit the least pulse broadening and have the greatest possible bandwidths, but in general are only usefully operated with single-mode sources.

In order to obtain a simple comparison for intermodal pulse broadening between multimode step index and multimode graded index fibers it is useful to consider the geometric optics picture for the two types of fiber.

3.10.1 Multimode step index fiber

Using the ray theory model, the fastest and slowest modes propagating in the step index fiber may be represented by the axial ray and the extreme meridional ray (which is incident at the core–cladding interface at the critical angle ϕ_c) respectively. The paths taken by these two rays in a perfectly structured step index fiber are shown in Figure 3.10. The delay difference between these two rays when travelling in the fiber core allows estimation of the pulse broadening resulting from intermodal dispersion within the fiber. As both rays are travelling at the same velocity within the constant refractive index fiber core, then the delay difference is directly related to their respective path lengths within the fiber. Hence the time taken for the axial ray to travel along a fiber of length L gives the minimum delay time T_{Min} and:

$$T_{\text{Min}} = \frac{distance}{velocity} = \frac{L}{(c/n_1)} = \frac{Ln_1}{c} \tag{3.20}$$

where n_1 is the refractive index of the core and c is the velocity of light in a vacuum.

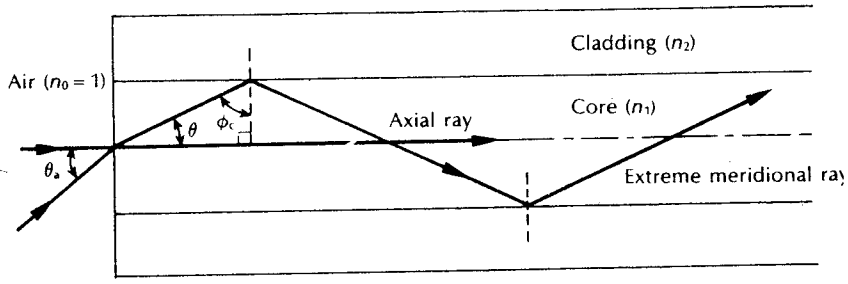

Figure 3.10 The paths taken by the axial and an extreme meridional ray in a perfect multimode step index fiber.

The extreme meridional ray exhibits the maximum delay time T_{Max} where:

$$T_{Max} = \frac{L/\cos\theta}{c/n_1} = \frac{Ln_1}{c\cos\theta} \tag{3.21}$$

Using Snell's law of refraction at the core–cladding interface following Eq. (2.2):

$$\sin\phi_c = \frac{n_2}{n_1} = \cos\theta \tag{3.22}$$

where n_2 is the refractive index of the cladding. Furthermore, substituting into Eq. (3.21) for $\cos\theta$ gives:

$$T_{Max} = \frac{Ln_1^2}{cn_2} \tag{3.23}$$

The delay difference δT_s between the extreme meridional ray and the axial ray may be obtained by subtracting Eq. (3.20) from Eq. (3.23). Hence:

$$\delta T_s = T_{Max} - T_{Min} = \frac{Ln_1^2}{cn_2} - \frac{Ln_1}{c}$$

$$= \frac{Ln_1^2}{cn_2}\left(\frac{n_1 - n_2}{n_1}\right) \tag{3.24}$$

$$\simeq \frac{Ln_1^2\Delta}{cn_2} \qquad \text{when } \Delta \ll 1 \tag{3.25}$$

where Δ is the relative refractive index difference. However, when $\Delta \ll 1$, then from the definition given by Eq. (2.9), the relative refractive index difference may also be given approximately by:

$$\Delta \simeq \frac{n_1 - n_2}{n_2} \tag{3.26}$$

Hence rearranging Eq. (3.24):

$$\delta T_s = \frac{Ln_1}{c}\left(\frac{n_1 - n_2}{n_2}\right) \simeq \frac{Ln_1\Delta}{c} \tag{3.27}$$

Also substituting for Δ from Eq. (2.10) gives:

$$\delta T_s \simeq \frac{L(NA)^2}{2n_1c} \tag{3.28}$$

where NA is the numerical aperture for the fiber. The approximate expressions for the delay difference given in Eq. (3.27) and (3.28) are usually employed to estimate the maximum pulse broadening in time due to intermodal dispersion in multimode step index fibers. It must be noted that this simple analysis only considers pulse broadening due to meridional rays and totally ignores skew rays with acceptance angles $\theta_{as} > \theta_a$ (see Section 2.2.4).

Again considering the perfect step index fiber, another useful quantity with regard to intermodal dispersion on an optical fiber link is the rms pulse broadening resulting from this dispersion mechanism along the fiber. When the optical input to the fiber is a pulse $p_i(t)$ of unit area, as illustrated in Figure 3.11, then [Ref. 37]:

$$\int_{-\infty}^{\infty} p_i(t)\, dt = 1 \tag{3.29}$$

It may be noted that $p_i(t)$ has a constant amplitude of $1/\delta T_s$ over the range

$$\frac{-\delta T_s}{2} \leqslant p(t) \leqslant \frac{\delta T_s}{2}$$

The rms pulse broadening at the fiber output due to intermodal dispersion for the multimode step index fiber σ_s (i.e. the standard deviation) may be given in terms of the variance σ_s^2 as (see Appendix C):

$$\sigma_s^2 = M_2 - M_1^2 \tag{3.30}$$

where M_1 is the first temporal moment which is equivalent to the mean value of the pulse and M_2, the second temporal moment, is equivalent to the mean square value of the pulse. Hence:

$$M_1 = \int_{-\infty}^{\infty} t p_i(t)\, dt \tag{3.31}$$

and

$$M_2 = \int_{-\infty}^{\infty} t^2 p_i(t)\, dt \tag{3.32}$$

The mean value M_1 for the unit input pulse of Figure 3.11 is zero, and assuming

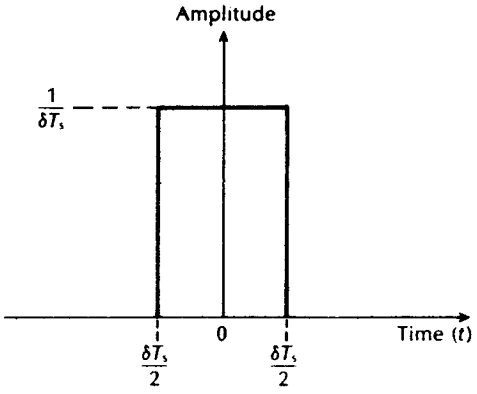

Figure 3.11 An illustration of the light input to the multimode step index fiber consisting of an ideal pulse or rectangular function with unit area.

this is maintained for the output pulse, then from Eqs. (3.30) and (3.32):

$$\sigma_s^2 = M_2 = \int_{-\infty}^{\infty} t^2 p_i(t)\, dt \tag{3.33}$$

Integrating over the limits of the input pulse (Figure 3.11) and substituting for $p_i(t)$ in Eq. (3.33) over this range gives:

$$\sigma_s^2 = \int_{-\delta T_s/2}^{\delta T_s/2} \frac{1}{\delta T_s} t^2\, dt$$

$$= \frac{1}{\delta T_s}\left[\frac{t^3}{3}\right]_{-\delta T_s/2}^{\delta T_s/2} = \frac{1}{3}\left(\frac{\delta T_s}{2}\right)^2 \tag{3.34}$$

Hence substituting from Eq. (3.27) for δT_s gives:

$$\sigma_s \simeq \frac{Ln_1\Delta}{2\sqrt{3}c} \simeq \frac{L(NA)^2}{4\sqrt{3}n_1 c} \tag{3.35}$$

Equation (3.35) allows estimation of the rms impulse response of a multimode step index fiber if it is assumed that intermodal dispersion dominates and there is a uniform distribution of light rays over the range $0 \leqslant \theta \leqslant \theta_a$. The pulse broadening is directly proportional to the relative refractive index difference Δ and the length of the fiber L. The latter emphasizes the bandwidth–length trade-off that exists, especially with multimode step index fibers, and which inhibits their use for wide-band long haul (between repeaters) systems. Furthermore, the pulse broadening is reduced by reduction of the relative refractive index difference Δ for the fiber. This suggests that weakly guiding fibers (see Section 2.4.1) with small Δ are best for low dispersion transmission. However, as may be seen from Eq. (3.35) this is also subject to a trade-off as a reduction in Δ reduces the acceptance angle θ_a and the NA, thus worsening the launch conditions.

Example 3.8

A 6 km optical link consists of multimode step index fiber with a core refractive index of 1.5 and a relative refractive index difference of 1%. Estimate:

(a) the delay difference between the slowest and fastest modes at the fiber output;
(b) the rms pulse broadening due to intermodal dispersion on the link;
(c) the maximum bit rate that may be obtained without substantial errors on the link assuming only intermodal dispersion;
(d) the bandwidth–length product corresponding to (c).

Solution: (a) The delay difference is given by Eq. (3.27) as:

$$\delta T_s \simeq \frac{Ln_1\Delta}{c} = \frac{6 \times 10^3 \times 1.5 \times 0.01}{2.998 \times 10^8}$$

$$= 300 \text{ ns}$$

(b) The rms pulse broadening due to intermodal dispersion may be obtained from Eq. (3.35) where:

$$\sigma_s = \frac{Ln_1\Delta}{2\sqrt{3}c} = \frac{1}{2\sqrt{3}} \frac{6 \times 10^3 \times 1.5 \times 0.01}{2.998 \times 10^8}$$

$$= 86.7 \text{ ns}$$

(c) The maximum bit rate may be estimated in two ways. Firstly, to get an idea of the maximum bit rate when assuming no pulse overlap Eq. (3.10) may be used where:

$$B_T(\max) = \frac{1}{2\tau} = \frac{1}{2\delta T_s} = \frac{1}{600 \times 10^{-9}}$$

$$= 1.7 \text{ Mbit s}^{-1}$$

Alternatively an improved estimate may be obtained using the calculated rms pulse broadening in Eq. (3.11) where

$$B_T(\max) = \frac{0.2}{\sigma_s} = \frac{0.2}{86.7 \times 10^{-9}}$$

$$= 2.3 \text{ Mbit s}^{-1}$$

(d) Using the most accurate estimate of the maximum bit rate from (c), and assuming return to zero pulses, the bandwidth–length product is

$$B_{opt} \times L = 2.3 \text{ MHz} \times 6 \text{ km} = 13.8 \text{ MHz km}$$

Intermodal dispersion may be reduced by propagation mechanisms within practical fibers. For instance, there is differential attenuation of the various modes in a step index fiber. This is due to the greater field penetration of the higher order modes into the cladding of the waveguide. These slower modes therefore exhibit larger losses at any core–cladding irregularities which tends to concentrate the transmitted optical power into the faster lower order modes. Thus the differential attenuation of modes reduces intermodal pulse broadening on a multimode optical link.

Another mechanism which reduces intermodal pulse broadening in nonperfect (i.e. practical) multimode fibers is the mode coupling or mixing discussed in Section 2.4.2. The coupling between guided modes transfers optical power from the slower to the faster modes, and vice versa. Hence, with strong coupling the optical power tends to be transmitted at an average speed, which is a mean of the various propagating modes. This reduces the intermodal dispersion on the link and makes it advantageous to encourage mode coupling within multimode fibers.

The expression for delay difference given in Eq. (3.27) for a perfect step index fiber may be modified for the fiber with mode coupling among all guided modes to

[Ref. 38]:

$$\delta T_{sc} \simeq \frac{n_1 \Delta}{c} (L L_c)^{\frac{1}{2}} \tag{3.36}$$

where L_c is a characteristic length for the fiber which is inversely proportional to the coupling strength. Hence, the delay difference increases at a slower rate proportional to $(LL_c)^{\frac{1}{2}}$ instead of the direct proportionality to L given in Eq. 3.27). However, the most successful technique for reducing intermodal dispersion in multimode fibers is by grading the core refractive index to follow a near parabolic profile. This has the effect of equalizing the transmission times of the various modes as discussed in the following section.

3.10.2 Multimode graded index fiber

Intermodal dispersion in multimode fibers is minimized with the use of graded index fibers. Hence, multimode graded index fibers show substantial bandwidth improvement over multimode step index fibers. The reason for the improved performance of graded index fibers may be observed by considering the ray diagram for a graded index fiber shown in Figure 3.12. The fiber shown has a parabolic index profile with a maximum at the core axis, as illustrated in Figure 3.12(a). Analytically, the index profile is given by Eq. (2.75) with $\alpha = 2$ as:

$$\begin{aligned} n(r) &= n_1(1 - 2\Delta(r/a)^2)^{\frac{1}{2}} \qquad r < a \text{ (core)} \\ &= n_1(1 - 2\Delta)^{\frac{1}{2}} = n_2 \qquad r \geqslant a \text{ (cladding)} \end{aligned} \tag{3.37}$$

Figure 3.12(b) shows several meridional ray paths within the fiber core. It may be observed that apart from the axial ray the meridional rays follow sinusoidal trajectories of different path lengths which result from the index grading, as was discussed in Section 2.4.4. However, following Eq. (2.40) the local group velocity

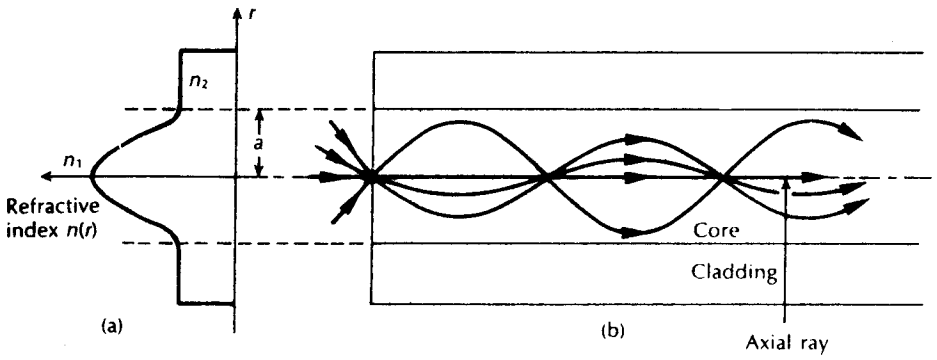

Figure 3.12 A multimode graded index fiber: (a) parabolic refractive index profile; (b) meridional ray paths within the fiber core.

is inversely proportional to the local refractive index and therefore the longer sinusoidal paths are compensated for by higher speeds in the lower index medium away from the axis. Hence there is an equalization of the transmission times of the various trajectories towards the transmission time of the axial ray which travels exclusively in the high index region at the core axis, and at the slowest speed. As these various ray paths may be considered to represent the different modes propagating in the fiber, then the graded profile reduces the disparity in the mode transit times.

The dramatic improvement in multimode fiber bandwidth achieved with a parabolic or near parabolic refractive index profile is highlighted by consideration of the reduced delay difference between the fastest and slowest modes for this graded index fiber δT_g. Using a ray theory approach the delay difference is given by [Ref. 39]:

$$\delta T_g \simeq \frac{L n_1 \Delta^2}{2c} \simeq \frac{(NA)^4}{8 n_1^3 c} \tag{3.38}$$

As in the step index case Eq. (2.10) is used for conversion between the two expressions shown.

However, a more rigorous analysis using electromagnetic mode theory gives an absolute temporal width at the fiber output of [Refs. 40, 41]:

$$\delta T_g = \frac{L n_1 \Delta^2}{8c} \tag{3.39}$$

which corresponds to an increase in transmission time for the slowest mode of $\Delta^2/8$ over the fastest mode. The expression given in Eq. (3.39) does not restrict the bandwidth to pulses with time slots corresponding to δT_g as 70% of the optical power is concentrated in the first half of the interval. Hence the rms pulse broadening is a useful parameter for assessment of intermodal dispersion in multimode graded index fibers. It may be shown [Ref. 41] that the rms pulse broadening of a near parabolic index profile graded index fiber σ_g is reduced compared to the similar broadening for the corresponding step index fiber σ_s (i.e. with the same relative refractive index difference) following:

$$\sigma_g = \frac{\Delta}{D} \sigma_s \tag{3.40}$$

where D is a constant between 4 and 10 depending on the precise evaluation and the exact optimum profile chosen.

The best minimum theoretical intermodal rms pulse broadening for a graded index fiber with an optimum characteristic refractive index profile for the core α_{op} of [Refs. 41, 42]:

$$\alpha_{op} = 2 - \frac{12\Delta}{5} \tag{3.41}$$

is given by combining Eqs. (3.27) and (3.40) as [Refs. 33, 42]:

$$\sigma_g = \frac{Ln_1\Delta^2}{20\sqrt{3}c} \tag{3.42}$$

Example 3.9

Compare the rms pulse broadening per kilometre due to intermodal dispersion for the multimode step index fiber of Example 3.8 with the corresponding rms pulse broadening for an optimum near parabolic profile graded index fiber with the same core axis refractive index and relative refractive index difference.

Solution: In Example 3.8, σ_s over 6 km of fiber is 86.7 ns. Hence the rms pulse broadening per kilometre for the multimode step index fiber is:

$$\frac{\sigma_s(1\text{ km})}{L} = \frac{86.7}{6} = 14.4\text{ ns km}^{-1}$$

Using Eq. (3.42), the rms pulse broadening per kilometre for the corresponding graded index fiber is:

$$\sigma_g(1\text{ km}) = \frac{Ln_1\Delta^2}{20\sqrt{3}c} = \frac{10^3 \times 1.5 \times (0.01)^2}{20\sqrt{3} \times 2.998 \times 10^8}$$

$$= 14.4\text{ ps km}^{-1}$$

Hence, from Example 3.9, the theoretical improvement factor of the graded index fiber in relation to intermodal rms pulse broadening is 1000. However, this level of improvement is not usually achieved in practice due to difficulties in controlling the refractive index profile radially over long lengths of fiber. Any deviation in the refractive index profile from the optimum results in increased intermodal pulse broadening. This may be observed from the curve shown in Figure 3.13, which gives the variation in intermodal pulse broadening (δT_g) as a function of the characteristic refractive index profile α for typical graded index fibers (where $\Delta = 1\%$). The curve displays a sharp minimum at a characteristic refractive index profile slightly less than 2 ($\alpha = 1.98$). This corresponds to the optimum value of α in order to minimize intermodal dispersion. Furthermore, the extreme sensitivity of the intermodal pulse broadening to slight variations in α from this optimum value is evident. Thus at present improvement factors for practical graded index fibers over corresponding step index fibers with regard to intermodal dispersion are around 100 [Ref. 40].

Another important factor in the determination of the optimum refractive index profile for a graded index fiber is the dispersion incurred due to the difference in refractive index between the fiber core and cladding. It results from a variation in the refractive index profile with optical wavelength in the graded fiber and is often given by a profile dispersion parameter $d\Delta/d\lambda$. Thus the optimized profile at a given

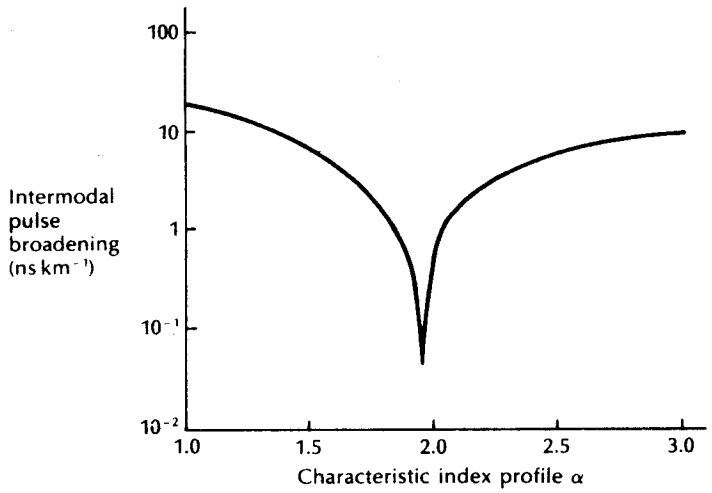

Figure 3.13 The intermodal pulse broadening δT_g for graded index fibers having $\Delta = 1\%$, versus the characteristic refractive index profile α.

wavelength is not necessarily optimized at another wavelength. As all optical fiber sources (e.g. injection lasers and light emitting diodes) have a finite spectral width, the profile shape must be altered to compensate for this dispersion mechanism. Moreover, the minimum overall dispersion for graded index fiber is also limited by the other intramodal dispersion mechanisms (i.e. material and waveguide dispersion). These give temporal pulse broadening of around 0.08 and 1 ns km^{-1} with injection lasers and light emitting diodes respectively. Therefore, practical pulse broadening values for graded index fibers lie in the range 0.2 to 1 ns km^{-1} This gives bandwidth–length products of between 0.5 and 2.5 GHz km when using lasers and optimum profile fiber.

3.10.3 Modal noise

The intermodal dispersion properties of multimode optical fibers (see Sections 3.10.1 and 3.10.2) create another phenomenon which affects the transmitted signals on the optical channel. It is exhibited within the speckle patterns observed in multimode fiber as fluctuations which have characteristic times longer than the resolution time of the detector, and is known as modal or speckle noise. The speckle patterns are formed by the interference of the modes from a coherent source when the coherence time of the source is greater than the intermodal dispersion time δT within the fiber. The coherence time for a source with uncorrelated source frequency width δf is simply $1/\delta f$. Hence, modal noise occurs when:

$$\delta f \gg \frac{1}{\delta T} \tag{3.43}$$

Disturbances along the fiber such as vibrations, discontinuities, connectors, splices and source/detector coupling may cause fluctuations in the speckle patterns and hence modal noise. It is generated when the correlation between two or more modes which gives the original interference is differentially delayed by these disturbances. The conditions which give rise to modal noise are therefore specified as:

(a) a coherent source with a narrow spectral width and long coherence length (propagation velocity multiplied by the coherence time);
(b) disturbances along the fiber which give differential mode delay or modal and spatial filtering;
(c) phase correlation between the modes.

Measurements [Ref. 43] of rms signal to modal noise ratio using good narrow linewidth injection lasers show large signal to noise ratio penalties under the previously mentioned conditions. The measurements were carried out by misaligning connectors to create disturbances. They gave carrier to noise ratios reduced by around 10 dB when the attenuation at each connector was 20 dB due to substantial axial misalignment.

Modal noise may be avoided by removing one of the conditions (they must all be present) which give rise to this degradation. Hence modal noise free transmission may be obtained by the following:

1. The use of a broad spectrum source in order to eliminate the modal interference effects. This may be achieved by either (a) increasing the width of the single longitudinal mode and hence decreasing its coherence time or (b) by increasing the number of longitudinal modes and averaging out of the interference patterns [Ref. 44].
2. In conjunction with 1(b) it is found that fibers with large numerical apertures support the transmission of a large number of modes giving a greater number of speckles, and hence reduce the modal noise generating effect of individual speckles [Ref. 45].
3. The use of single-mode fiber which does not support the transmission of different modes and thus there is no intermodal interference.
4. The removal of disturbances along the fiber. This has been investigated with regard to connector design [Ref. 46] in order to reduce the shift in speckle pattern induced by mechanical vibration and fiber misalignment.

Hence, modal noise may be prevented on an optical fiber link through suitable choice of the system components. However, this may not always be possible and then certain levels of modal noise must be tolerated. This tends to be the case on high quality analog optical fiber links where multimode injection lasers are frequently used. Analog transmission is also more susceptible to modal noise due to the higher optical power levels required at the receiver when quantum noise effects are considered (see Section 9.2.5). Therefore, it is important that modal noise is taken into account within the design considerations for these systems.

Modal noise, however, can be present in single-mode fiber links when propagation of the two fundamental modes with orthogonal polarization is allowed or, alternatively, when the second order modes* are not sufficiently attenuated. The former modal noise type, which is known as polarization modal noise, is outlined in Section 3.13.1. For the latter type, it is apparent that at shorter wavelengths, a nominally single-mode fiber can also guide four second order LP modes (see Section 2.4.1). Modal noise can therefore be introduced into single-mode fiber systems by time-varying interference between the LP_{01} and the LP_{11} modes when the fiber is operated at a wavelength which is smaller than the cutoff wavelength of the second order modes. The effect has been observed in overmoded single-mode fibers [Ref. 47] and may be caused by a number of conditions. In particular the insertion of a short jumper cable or repair section, with a lateral offset, in a long single-mode fiber can excite the second order LP_{11} mode [Ref. 41]. Moreover, such a repair section can also attenuate the fundamental LP_{01} mode if its operating wavelength is near the cutoff wavelength for this mode. Hence to reduce modal noise, repair sections should use special fibers with a lower value of cutoff wavelength than that in the long single-mode fiber link; also offsets at joints should be minimized.

3.11 Overall fiber dispersion

3.11.1 Multimode fibers

The overall dispersion in multimode fibers comprises both intramodal and intermodal terms. The total rms pulse broadening σ_T is given (see Appendix D) by:

$$\sigma_T = (\sigma_c^2 + \sigma_n^2)^{\frac{1}{2}} \tag{3.44}$$

where σ_c is the intramodal or chromatic broadening and σ_n is the intermodal broadening caused by delay differences between the modes (i.e. σ_s for multimode step index fiber and σ_g for multimode graded index fiber). The intramodal term σ_c consists of pulse broadening due to both material and waveguide dispersion. However, since waveguide dispersion is generally negligible compared with material dispersion in multimode fibers, then $\sigma_c \simeq \sigma_m$.

Example 3.10

A multimode step index fiber has a numerical aperture of 0.3 and a core refractive index of 1.45. The material dispersion parameter for the fiber is 250 ps nm^{-1} km^{-1} which makes material dispersion the totally dominating intramodal dispersion mechanism. Estimate (a) the total rms pulse broadening per kilometre when the

* In addition to the two orthogonal LP_{01} modes, at shorter wavelengths 'single-mode' fiber can propagate four LP_{11} modes.

fiber is used with an LED source of rms spectral width 50 nm and (b) the corresponding bandwidth–length product for the fiber.

Solution: (a) The rms pulse broadening per kilometre due to material dispersion may be obtained from Eq. (3.18), where

$$\sigma_m(1\text{ km}) \simeq \frac{\sigma_\lambda L \lambda}{c}\left|\frac{d^2 n_1}{d\lambda^2}\right| = \sigma_\lambda LM = 50 \times 1 \times 250\text{ ps km}^{-1}$$
$$= 12.5\text{ ns km}^{-1}$$

The rms pulse broadening per kilometre due to intermodal dispersion for the step index fiber is given by Eq. (3.35) as:

$$\sigma_s(1\text{ km}) \simeq \frac{L(NA)^2}{4\sqrt{3}n_1 c} = \frac{10^3 \times 0.09}{4\sqrt{3} \times 1.45 \times 2.998 \times 10^8}$$
$$= 29.9\text{ ns km}^{-1}$$

The total rms pulse broadening per kilometre may be obtained using Eq. (3.43), where $\sigma_c \approx \sigma_m$ as the waveguide dispersion is negligible and $\sigma_n = \sigma_s$ for the multimode step index fiber. Hence:

$$\sigma_T = (\sigma_m^2 + \sigma_s^2)^{\frac{1}{2}} = (12.5^2 + 29.9^2)^{\frac{1}{2}}$$
$$= 32.4\text{ ns km}^{-1}$$

(b) The bandwidth–length product may be estimated from the relationship given in Eq. (3.11) where:

$$B_{opt} \times L = \frac{0.2}{\sigma_T} = \frac{0.2}{32.4 \times 10^{-9}}$$
$$= 6.2\text{ MHz km}$$

3.11.2 Single-mode fibers

The pulse broadening in single-mode fibers results almost entirely from intramodal or chromatic dispersion as only a single-mode is allowed to propagate.* Hence the bandwidth is limited by the finite spectral width of the source. Unlike the situation in multimode fibers, the mechanisms giving intramodal dispersion in single-mode fibers tend to be interrelated in a complex manner. The transit time or specific group delay τ_g for a light pulse propagating along a unit length of single-mode fiber may be given, following Eq. (2.107), as:

$$\tau_g = \frac{1}{c}\frac{d\beta}{dk} \tag{3.45}$$

where c is the velocity of light in a vacuum, β is the propagation constant for a

* Polarization mode dispersion can, however, occur in single-mode fibers (see Section 3.13.1).

mode within the fiber core of refractive index n_1 and k is the propagation constant for the mode in a vacuum.

The total first order dispersion parameter or the chromatic dispersion of a single-mode fiber, D_T, is given by the derivative of the specific group delay with respect to the vacuum wavelength λ as:

$$D_T = \frac{d\tau_g}{d\lambda} \tag{3.46}$$

In common with the material dispersion parameter it is usually expressed in units of ps nm^{-1} km^{-1}. When the variable λ is replaced by ω, then the total dispersion parameter becomes:

$$D_T = -\frac{\omega}{\lambda}\frac{d\tau_g}{d\omega} = -\frac{\omega}{\lambda}\frac{d^2\beta}{d\omega^2} \tag{3.47}$$

The fiber exhibits intramodal dispersion when β varies nonlinearly with wavelength. From Eq. (2.71) β may be expressed in terms of the relative refractive index difference Δ and the normalized propagation constant b as:

$$\beta = kn_1[1 - 2\Delta(1 - b)]^{\frac{1}{2}} \tag{3.48}$$

The rms pulse broadening caused by intramodal dispersion down a fiber of length L is given by the derivative of the group delay with respect to wavelength as [Ref. 27]:

$$\text{Total rms pulse broadening} = \sigma_\lambda L\left|\frac{d\tau_g}{d\lambda}\right| = \frac{\sigma_\lambda L 2\pi}{c\lambda^2}\frac{d^2\beta}{dk^2} \tag{3.49}$$

where σ_λ is the source rms spectral linewidth centred at a wavelength λ.

When Eq. (3.44) is substituted into Eq. (3.45), detailed calculation of the first and second derivatives with respect to k gives the dependence of the pulse broadening on the fiber material's properties and the normalized propagation constant b. This gives rise to three interrelated effects which involve complicated cross-product terms. However, the final expression may be separated into three composite dispersion components in such a way that one of the effects dominates each term [Ref. 50]. The dominating effects are as follows:

1. The material dispersion parameter D_M defined by $\lambda/c\,|\,d^2n/d\lambda^2\,|$ where $n = n_1$ or n_2 for the core or cladding respectively.

2. The waveguide dispersion parameter D_W, which may be obtained from Eq. (3.47) by substitution from Eq. (2.114) for τ_g, is defined as:*

$$D_W = -\left(\frac{n_1 - n_2}{\lambda c}\right) V \frac{d^2(Vb)}{dV^2} \tag{3.50}$$

where V is the normalized frequency for the fiber. Since the normalized propagation constant b for a specific fiber is only dependent on V, then the normalized waveguide dispersion coefficient $V\,d^2(Vb)/dV^2$ also depends on V. This latter function is another universal parameter which plays a central role in the theory of single-mode fibers.

3. A profile dispersion parameter D_P which is proportional to $d\Delta/d\lambda$.

This situation is different from multimode fibers where the majority of modes propagate far from cutoff and hence most of the power is transmitted in the fiber core. In the multimode case the composite dispersion components may be simplified and separated into two intramodal terms which depend on either material or waveguide dispersion, as was discussed in Section 3.9. Also, especially when considering step index multimode fibers, the effect of profile dispersion is negligible. Although material and waveguide dispersion tend to be dominant in single-mode fibers, the composite profile should not be ignored. However, the profile dispersion parameter D_P can be quite small (e.g. less than 0.5 ps nm^{-1} km^{-1}), especially at long wavelengths and hence is often neglected in rough estimates of total dispersion within single-mode fibers.

Strictly speaking, in single-mode fiber with a power law refractive index profile the composite dispersion terms should be employed [Ref. 51]. Nevertheless, it is useful to consider the total first order dispersion D_T in a practical single-mode fiber as comprising:

$$D_T = D_M + D_W + D_P \qquad (\text{ps nm}^{-1}\,\text{km}^{-1}) \tag{3.51}$$

which is simply the addition of the material dispersion D_M, the waveguide dispersion D_W and the profile dispersion D_P components. However, in standard single-mode fibers the total dispersion tends to be dominated by the material dispersion of fused silica. This parameter is shown plotted against wavelength in Figure 3.9. It may be observed that the characteristic goes through zero at a wavelength of 1.27 μm. This zero material dispersion (ZMD) point can be shifted anywhere in the wavelength range 1.2 to 1.4 μm by the addition of suitable dopants [Ref. 52]. For instance, the ZMD point shifts from 1.27 μm to approximately 1.37 μm as the GeO_2 dopant concentration is increased from 0 to 15%. However, the ZMD point alone does not represent a point of zero pulse broadening since the pulse dispersion is influenced by both waveguide and profile dispersion.

* Equation (3.50) does not provide the composite waveguide dispersion term (i.e. taking into account both the fiber core and the cladding) from which it differs by a factor near unity which contains $dn_2/d\lambda$ [Ref. 51].

With zero material dispersion the pulse spreading is dictated by the waveguide dispersion coefficient $V\,d^2(Vb)/dV^2$, which is illustrated in Figure 3.14 as a function of normalized frequency for the LP_{01} mode. It may be seen that in the single-mode region where the normalized frequency is less than 2.405 (see Section 2.5) the waveguide dispersion is always positive and has a maximum at $V = 1.15$. In this case the waveguide dispersion goes to zero outside the true single-mode region at $V = 3.0$. However, a change in the fiber parameters (such as core radius) or in the operating wavelength alters the normalized frequency and therefore the waveguide dispersion.

The total fiber dispersion, which depends on both the fiber material composition and dimensions, may be minimized by trading off material and waveguide dispersion whilst limiting the profile dispersion (i.e. restricting the variation in refractive index with wavelength). For wavelengths longer than the ZMD point, the material dispersion parameter is positive whereas the waveguide dispersion parameter is negative, as shown in Figure 3.15. However, the total dispersion D_T is approximately equal to the sum of the material dispersion D_M and the waveguide dispersion D_W following Eq. (3.50). Hence for a particular wavelength, designated λ_0, which is slightly larger than the ZMD point wavelength, the waveguide dispersion compensates for the material dispersion and the total first order dispersion parameter D_T becomes zero (See Figure 3.15). The wavelength at which the first order dispersion is zero λ_0 may be selected in the range 1.3 to 2 μm by careful control of the fiber core diameter and profile [Ref. 50]. This point is illustrated in Figure 3.16 where the total first order dispersion as a function of

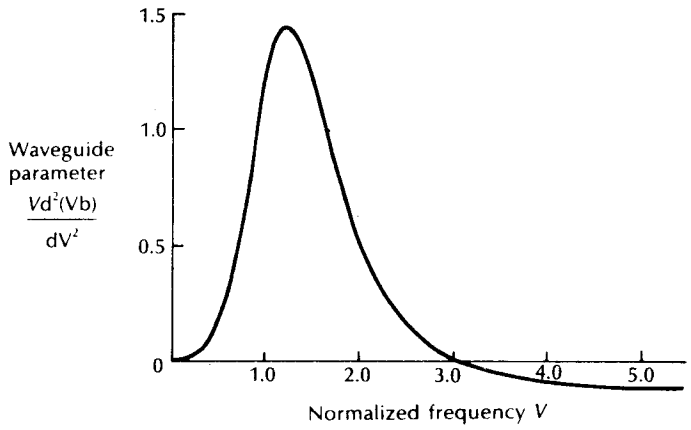

Figure 3.14 The waveguide parameter $Vd^2(Vb)/dV^2$ as a function of the normalized frequency V for the LP_{01} mode. Reproduced with permission from W. A. Gambling. A. H. Hartog and C. M. Ragdale, *The Radio and Electron. Eng* **51**, p. 313, 1981.

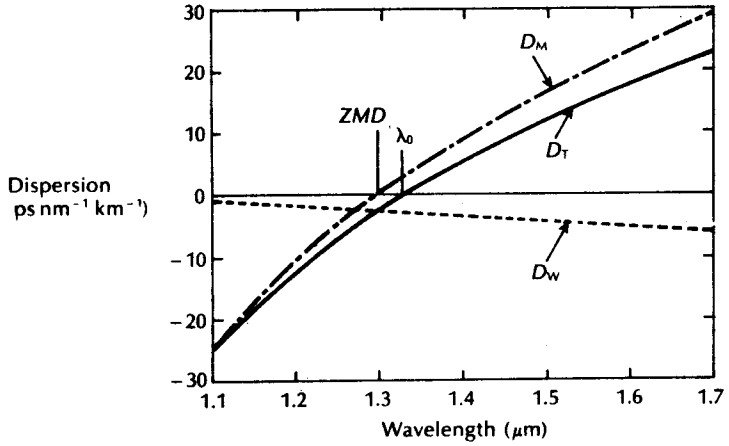

Figure 3.15 The material dispersion parameter (D_M), the waveguide dispersion parameter (D_W) and the total dispersion parameter (D_T) as functions of wavelength for a conventional single-mode fiber.

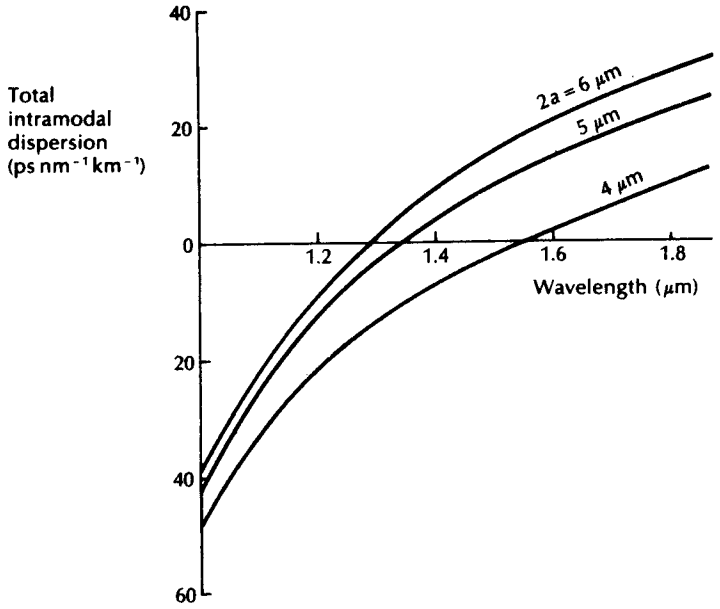

Figure 3.16 The total first order intramodal dispersion as a function of wavelength for single-mode fibers with core diameters of 4, 5, and 6 μm. Reproduced with permission from W. A. Gambling. A. H. Hartog, and C. M. Ragdale, *The Radio and Electron. Eng.*, **51**, p. 313, 1981.

wavelength is shown for three single-mode fibers with core diameters of 4, 5 and 6 μm.

The effect of the interaction of material and waveguide dispersion on λ_0 is also demonstrated in the dispersion against wavelength characteristics for a single-mode silica core fiber shown in Figure 3.17. It may be noted that the ZMD point occurs at a wavelength of 1.27 μm but that the influence of waveguide dispersion shifts the total dispersion minimum towards the longer wavelength giving a λ_0 of 1.32 μm.

The wavelength at which the first order dispersion is zero λ_0 may be extended to

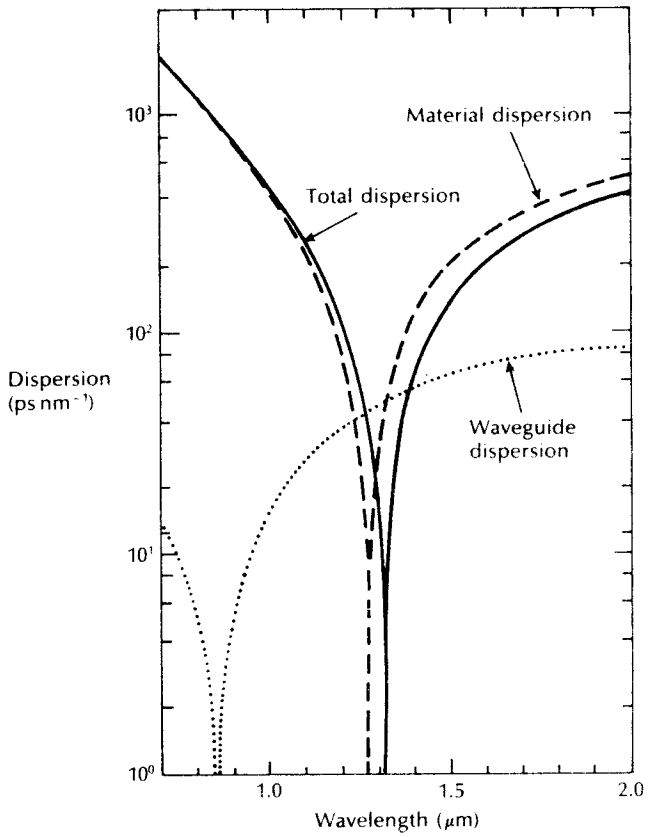

Figure 3.17 The pulse dispersion as a function of wavelength in 11 km single mode fiber showing the major contributing dispersion mechanisms (dashed and dotted curves) and the overall dispersion (solid curve). Reproduced with permission from J. I. Yamada, M. Saruwatari, K. Asatani, H. Tsuchiya, A. Kawana, K. Sugiyama and T. Kumara, 'High speed optical pulse transmission at 1.29 μm wavelength using low-loss single-mode fibers' *IEEE J. Quantum Electron.*, **QE-14** p. 791, 1978. Copyright © 1980, IEEE.

wavelengths of 1.55 μm and beyond by a combination of three techniques. These are:

(a) lowering the normalized frequency (V value) for the fiber;
(b) increasing the relative refractive index difference Δ for the fiber;
(c) suitable doping of the silica with germanium.

This allows bandwidth–length products for such single-mode fibers to be in excess of 100 GHz km^{-1} [Ref. 53] at the slight disadvantage of increased attenuation due to Rayleigh scattering within the doped silica.

For single-mode fibers optimized for operation at a wavelength of 1.3 μm, the CCITT* [Ref. 54] recommends that the maximum value of chromatic dispersion D_T shall not exceed 3.5 ps nm^{-1} km^{-1} in the wavelength range 1.285 to 1.330 μm. Moreover, for the same fiber D_T should be less than 20 ps nm^{-1} km^{-1} at the wavelength of 1.55 [Ref. 55]. Hence, although the wavelength of zero first order chromatic dispersion (i.e. $D_T = 0$) is often called the zero-dispersion wavelength, it is more correct to refer to it as the wavelength of minimum dispersion because of the significant second order dispersion effects.

The variation of the intramodal dispersion with wavelength is usually characterized by the second order dispersion parameter or dispersion slope S which may be written as [Ref. 56]:

$$S = \frac{dD_T}{d\lambda} = \frac{d^2\tau_g}{d\lambda^2} \tag{3.52}$$

Whereas the first order dispersion parameter D_T may be seen to be related only to the second derivative of the propagation constant β with respect to angular frequency in Eq. (3.47), the dispersion slope can be shown to be related to both the second and third derivatives [Ref. 51] following:

$$S = \frac{(2\pi c)^3}{\lambda^4}\frac{d^3\beta}{d\omega^3} + \frac{4\pi c}{\lambda^3}\frac{d^2\beta}{d\omega^2} \tag{3.53}$$

It should be noted that although there is zero first order dispersion at λ_0, these higher order chromatic effects impose limitations on the possible bandwidths that may be achieved with single-mode fibers. For example, a fundamental lower limit to pulse spreading in silica-based fibers of around 2.50×10^{-2} ps nm^{-1} km^{-1} is suggested at a wavelength of 1.273 μm [Ref. 57]. These secondary effects such as birefringence arising from ellipticity or mechanical stress in the fiber core are considered further in Section 3.13. However, they may cause dispersion, especially in the case of mechanical stress of between 2 and 40 ps km^{-1}. If mechanical stress is avoided, pulse dispersion around the lower limit may be obtained in the longer wavelength region (i.e. 1.3 to 1.7 μm). By contrast the minimum pulse spread at a wavelength of 0.85 μm is around 100 ps nm^{-1} km^{-1} [Ref. 39].

* CCITT Recommendation G.652.

An important value of the dispersion slope $S(\lambda)$ is obtained at the wavelength of minimum intramodal dispersion λ_0 such that:

$$S_0 = S(\lambda_0) \tag{3.54}$$

where S_0 is called the zero-dispersion slope which, from Eqs. (3.46) and (3.52), is determined only by the third derivative of β. Typical values for the dispersion slope for standard single-mode fiber at λ_0 are in the region 0.085 to 0.092 ps nm^{-2} km^{-1} Moreover, for such fibers the CCITT has recently proposed that λ_0 lies in the range 1.295 to 1.322 μm with S_0 less than 0.095 ps nm^{-2} km^{-1} [Ref. 58]. The total chromatic dispersion at an arbitrary wavelength can be estimated when the two parameters λ_0 and S_0 are specified according to [Ref. 55]:

$$D_T(\lambda) = \frac{\lambda S_0}{4}\left[1 - \left(\frac{\lambda_0}{\lambda}\right)^4\right] \tag{3.55}$$

Example 3.11

A typical single-mode fiber has a zero-dispersion wavelength of 1.31 μm with a dispersion slope of 0.09 ps nm^{-2} km^{-1}. Compare the total first order dispersion for the fiber at the wavelengths of 1.28 μm and 1.55 μm. When the material dispersion and profile dispersion at the latter wavelength are 13.5 ps nm^{-1} km^{-1} and 0.4 ps nm^{-1} km^{-1}, respectively, determine the waveguide dispersion at this wavelength.

Solution: The total first order dispersion for the fiber at the two wavelengths may be obtained from Eq. (3.55). Hence:

$$D_T(1280\text{ nm}) = \frac{\lambda S_0}{4}\left[1 - \left(\frac{\lambda_0}{\lambda}\right)^4\right]$$

$$= \frac{1280 \times 0.09 \times 10^{-12}}{4}\left[1 - \left(\frac{1310}{1280}\right)^4\right]$$

$$= -2.8 \text{ ps nm}^{-1}\text{ km}^{-1}$$

and

$$D_T(1550\text{ nm}) = \frac{1550 \times 0.09 \times 10^{-12}}{4}\left[1 - \left(\frac{1310}{1550}\right)^4\right]$$

$$= 17.1 \text{ ps nm}^{-1}\text{ km}^{-1}$$

The total dispersion at the 1.28 μm wavelength exhibits a negative sign due to the influence of the waveguide dispersion. Furthermore, as anticipated the total dispersion at the longer wavelength (1.55 μm) is considerably greater than that obtained near the zero-dispersion wavelength.

The waveguide dispersion for the fiber at a wavelength of 1.55 μm is given by Eq. (3.51) where:

$$\begin{aligned} D_W &= D_T - (D_M + D_P) \\ &= 17.1 - (13.5 + 0.4) \\ &= 3.2 \text{ ps nm}^{-1} \text{km}^{-1} \end{aligned}$$

3.12 Dispersion modified single-mode fibers

It was suggested in Section 3.11.2 that it is possible to modify the dispersion characteristics of single-mode fibers by the tailoring of specific fiber parameters. However, the major trade-off which occurs in this process between material dispersion (Eq. 3.19) and waveguide dispersion (Eq.3.50) may be expressed as:

$$D_T = D_M + D_W = \underbrace{\frac{\lambda}{c}\left|\frac{d^2 n_1}{d\lambda^2}\right|}_{\text{material dispersion}} - \underbrace{\left[\frac{n_1 - n_2}{\lambda c}\right]\frac{V d^2(Vb)}{dV^2}}_{\text{waveguide dispersion}} \tag{3.56}$$

At wavelengths longer than the zero material dispersion (ZMD) point in most common fiber designs, the D_M and D_W components are of opposite sign and can therefore be made to cancel at some longer wavelength. Hence the wavelength of zero first order chromatic dispersion can be shifted to the lowest loss wavelength for silicate glass fibers at 1.55 μm to provide both low dispersion and low loss fiber. This may be achieved by such mechanisms as a reduction in the fiber core diameter with an accompanying increase in the relative or fractional index difference to create so-called dispersion shifted (DS) single-mode fibers. However, the design flexibility required to obtain particular dispersion, attenuation, mode-field diameter and bend loss characteristics has resulted in specific, different refractive index profiles for these dispersion modified fibers.

An alternative modification of the dispersion characteristics of single-mode fibers involves the achievement of a low dispersion window over the low loss wavelength region between 1.3 μm and 1.6 μm. Such fibers, which relax the spectral requirements for optical sources and allow flexible wavelength division multiplexing (see Section 11.9.3) are known as dispersion flattened (DF) single-mode fibers. In order to obtain DF fibers multilayer index profiles are fabricated with increased waveguide dispersion which is tailored to provide overall dispersion (e.g. less than 2 ps nm^{-1} km^{-1}) over the entire wavelength range 1.3 to 1.6 μm [Ref. 59]. In effect these fibers exhibit two wavelengths of zero total chromatic dispersion. This factor may be observed in Figure 3.18 which shows the overall dispersion characteristics as a function of optical wavelength for standard single-mode fiber optimized for operation at 1.3 μm in comparison with both DS and DF fiber [Ref. 60].

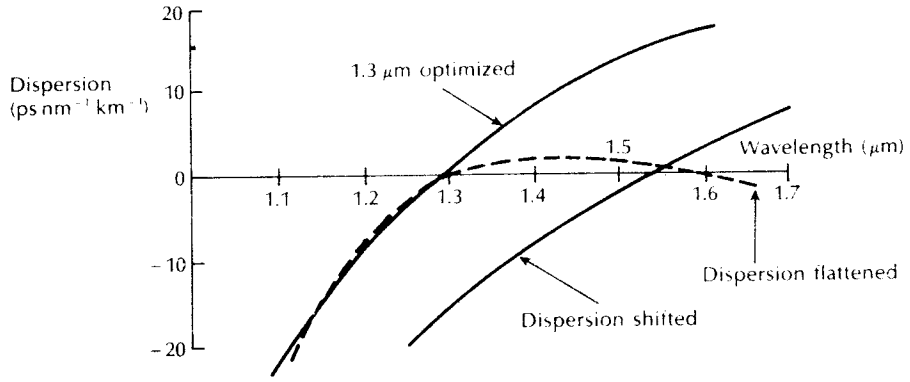

Figure 3.18 Total dispersion characteristics for the various types of single-mode fiber.

3.12.1 Dispersion shifted fibers

A wide variety of single-mode fiber refractive index profiles are capable of modification in order to tune the zero-dispersion wavelength point λ_0 to a specific wavelength within a region adjacent to the zero-material-dispersion (ZMD) point. In the simplest case, the step index profile illustrated in Figure 3.19 gives a shift to longer wavelength by reducing the core diameter and increasing the fractional index difference. Typical values for the two parameters are 4.4 μm and 0.012 respectively [Ref. 61]. For comparison, the standard nonshifted design is shown dotted in Figure 3.19.

It was indicated in Section 3.11.2 that λ_0 could be shifted to longer wavelength by altering the material composition of the single-mode fiber. For suitable power confinement of the fundamental mode, the normalized frequency V should be maintained in the range 1.5 to 2.4 μm and the fractional index difference must be increased as a square function whilst the core diameter is linearly reduced to keep V constant. This is normally achieved by substantially increasing the level of germanium doping in the fiber core. Figure 3.20 [Ref. 61] displays typical material and waveguide dispersion characteristics for single-mode step index fibers with various compositions and core radii. It may be observed that higher concentrations of the dopant cause a shift to longer wavelength which when coupled with a reduction in the mode-field diameter (MFD), giving a larger value (negative of waveguide dispersion), leads to the shifted fiber characteristic shown in Figure 3.20.

A problem that arises with the simple step index approach to dispersion shifting displayed in Figure 3.19 is that the fibers produced exhibit relatively high dopant dependent losses at operation wavelengths around 1.55 μm. This excess optical loss, which may be of the order of 2 dB km^{-1}, [Ref. 61] could be caused by stress-induced defects which occur in the region of the core–cladding interface [Ref. 62]. Alternatively, it may result from refractive index inhomogeneities associated with waveguide variations at the core–cladding interface [Ref. 63]. A logical assumption

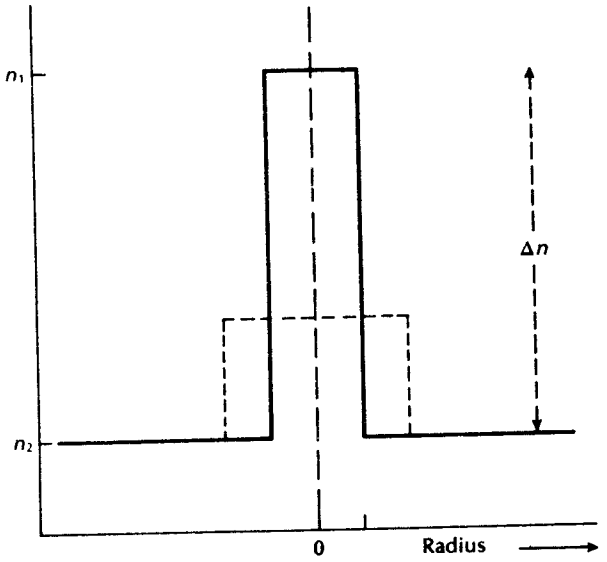

Figure 3.19 Refractive index profile of a step index dispersion shifted fiber (solid) with a conventional nonshifted profile design (dashed).

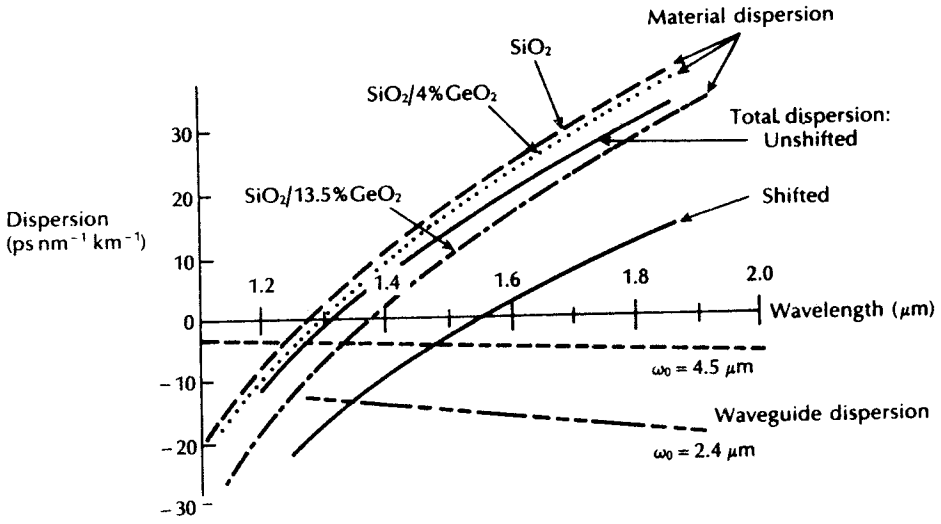

Figure 3.20 Material, waveguide and total dispersion characteristics for conventional and dispersion shifted step index single-mode fibers showing variation with composition and spot size (ω_0).

is that any stress occurring across the core–cladding interface might be reduced by grading the material composition and therefore an investigation of graded index single-mode fiber designs was undertaken.

Several of the graded refractive index profile DS fiber types are illustrated in Figure 3.21. The triangular profile shown in Figure 3.21(a) is the simplest and was the first to exhibit the same low loss (i.e. 0.24 dB km^{-1}) at a wavelength of 1.56 μm (i.e. λ_0) as conventional nonshifted single-mode fiber [Ref. 64]. Furthermore, such fiber designs also provide an increased MFD over equivalent step index structures which assists with fiber splicing [Ref. 61]. However, in the basic triangular profile design the optimum parameters giving low loss together with zero dispersion at a wavelength of 1.55 μm cause the LP_{11} mode to cutoff in the wavelength region 0.85 to 0.9 μm. Thus the fiber must be operated far from cutoff which produces

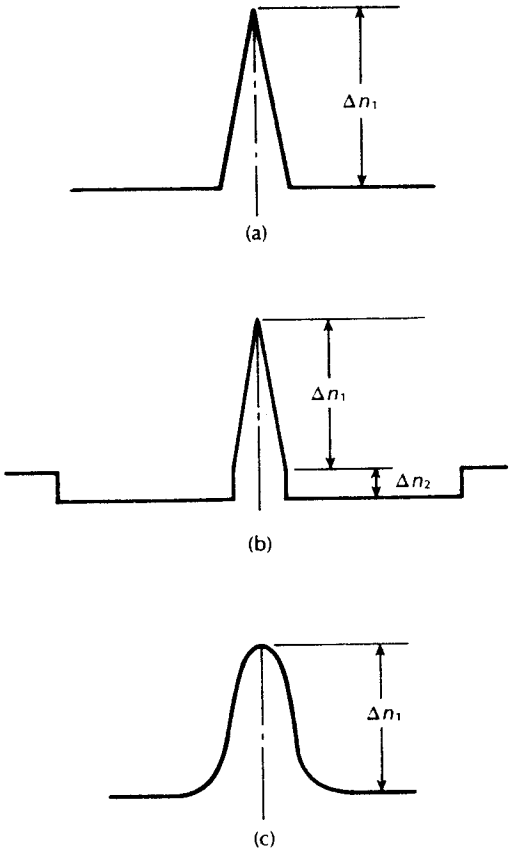

Figure 3.21 Refractive index profiles for graded index dispersion shifted fibers: (a) triangular profile; (b) depressed-cladding triangular profile; (c) Gaussian profile.

sensitivity to bend induced losses (in particular microbending) at the 1.55 μm wavelength [Ref. 65]. One method to overcome this drawback is to employ a triangular index profile combined with a depressed cladding index, as shown in Figure 3.21(b) [Ref. 66]. In this case the susceptibility to microbending losses is reduced through a shift of the LP_{11} cutoff wavelength to around 1.1 μm with a MFD of 7 μm at 1.55 μm.

Low losses and zero dispersion at a wavelength of 1.55 μm have also been obtained with a Gaussian refractive index profile, as illustrated in Figure 3.21(c). This profile, which was achieved using the vapour axial deposition fabrication process (see Section 4.4.2), produced losses of 0.21 dB km^{-1} at the λ_0 wavelength of 1.55 μm [Ref. 67].

The alternative approach for the production of DS single-mode fiber has involved the use of multiple index designs. One such fiber type which has been used to demonstrate dispersion shifting but which has been more widely employed for DF fibers (see Section 3.12.2) is the doubly clad or W fiber (see Section 2.5). However the multiple index triangular profile fibers [Ref. 68] and the segmented-core triangular profile designs [Ref. 69] which are shown in Figure 3.22(a) and (b), respectively, have reduced the sensitivity to microbending by shifting the LP_{11} mode cutoff to longer wavelength whilst maintaining a MFD of around 9 μm at a wavelength of 1.55 μm. The latter technique of introducing a ring of elevated index around the triangular core enhances the guidance of the LP_{11} mode towards longer wavelength. Such fibers may be obtained as commercial products and have been utilized within the telecommunication network [Ref. 70], exhibiting losses as low as 0.17 dB at 1.55 μm [Ref. 71].

More recently, dual-shaped core DS fibers have come under investigation in order to provide an improvement in bend loss performance over the 1.55 μm wavelength region [Refs. 72, 73]. A dual-shape core refractive index profile is shown in Figure 3.22(c), which illustrates a step index fiber design. However, several graded

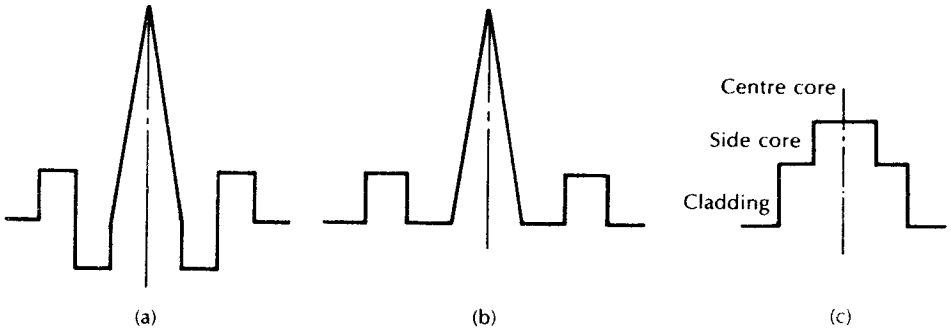

Figure 3.22 Advanced refractive index profiles for dispersion shifted fibers (a) triangular profile multiple index design; (b) segmented-core triangular profile design; (c) dual-shaped core design.

index profiles have also been studied in relation to improvements in bend loss characteristics without the incursion of increases in splice loss when the fibers are jointed [Ref. 73].

3.12.2 Dispersion flattened fibers

The original W fiber structure mentioned in Section 3.12.1 was initially employed to modify the dispersion characteristics of single-mode fibers in order to give two wavelengths of zero dispersion, as illustrated in Figure 3.18. A typical W fiber index profile (double clad) is shown in Figure 3.23(a). The first practical demonstration of dispersion flattening using the W structure was reported in 1981 [Ref. 74]. However, drawbacks with the W structural design included the requirement for a high degree of dimensional control so as to make reproducible DF fibers [Ref. 75], comparatively high overall fiber losses (around 0.3 dB km^{-1}), as well as a very high sensitivity to fiber bend losses. The latter factor results from operation very close to the cutoff (or leakage) of the fundamental mode in the long wavelength window in order to obtain a flat dispersion characteristic.

To reduce the sensitivity to bend losses associated with the W fiber structure the light which penetrates into the outer cladding area can be retrapped by introducing a further region of raised index into the structure. This approach has resulted in the triple clad (TC) and quadruple clad (QC) structures shown in Figure 3.23(b) and (c) [Refs. 76, 77]. An independent but similar program produced segmented-core DF fiber designs [Ref. 71]. Reports of low attenuation of 0.19 dB km^{-1} for DF single-mode fiber at a wavelength of 1.55 μm [Ref. 78] with significantly reduced bending losses [Ref. 79] have been made. In addition, mean splice losses of 0.04 to 0.05 dB have been achieved for MFDs of typically 6 μm and 7 μm at the 1.3 μm and 1.55 μm wavelengths respectively [Ref. 78]. However, although it is suggested [Ref. 58] that efforts remain directed towards improvements in the reduction of bend loss sensitivity and the identification of the optimum MFD, it is the case that certain DF single-mode fibers have been transferred in production [Ref. 73]. Nevertheless, it is likely that their eventual use within the telecommunications network will depend upon their performance, cost and compatibility in relation to conventional (i.e. 1.3 μm dispersion optimized) single-mode fiber.

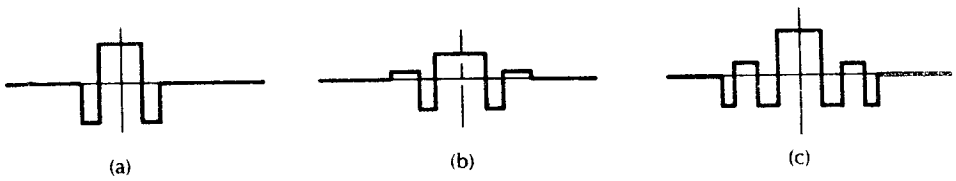

Figure 3.23 Dispersion flattened fiber refractive index profiles: (a) double clad fiber (*W* fiber); (b) triple clad fiber; (c) quadruple clad fiber.

3.13 Polarization

Cylindrical optical fibers do not generally maintain the polarization state of the light input for more than a few metres, and hence for many applications involving optical fiber transmission some form of intensity modulation (see Section 7.5) of the optical source is utilized. The optical signal is thus detected by a photodiode which is insensitive to optical polarization or phase of the light wave within the fiber. Nevertheless, systems and applications have been investigated [Ref. 81] (see Sections 12.1 and 14.5.1) which could require the polarization states of the input light to be maintained over significant distances, and fibers have been designed for this purpose. These fibers are single-mode and the maintenance of the polarization state is described in terms of a phenomenon known as modal birefringence.

3.13.1 Modal birefringence

Single-mode fibers with nominal circular symmetry about the core axis allow the propagation of two nearly degenerate modes with orthogonal polarizations. They are therefore bimodal supporting HE_{11}^{x} and HE_{11}^{y} modes where the principal axes x and y are determined by the symmetry elements of the fiber cross section. Thus the fiber behaves as a birefringent medium due to the difference in the effective refractive indices, and hence phase velocities, for these two orthogonally polarized modes. The modes therefore have different propagation constants β_x and β_y which are dictated by the anisotropy of the fiber cross section. When the fiber cross section is independent of the fiber length L in the z direction, then the modal birefringence B_F for the fiber is given by [Ref. 82]:

$$B_F = \frac{(\beta_x - \beta_y)}{(2\pi/\lambda)} \tag{3.57}$$

where λ is the optical wavelength. Light polarized along one of the principal axes will retain its polarization for all L.

The difference in phase velocities causes the fiber to exhibit a linear retardation $\Phi(z)$ which depends on the fiber length L in the z direction and is given by [Ref. 82]:

$$\Phi(z) = (\beta_x - \beta_y)L \tag{3.58}$$

assuming that the phase coherence of the two mode components is maintained The phase coherence of the two mode components is achieved when the delay between the two transit times is less than the coherence time of the source. As indicated in Section 3.11 the coherence time for the source is equal to the reciprocal of the uncorrelated source frequency width ($1/\delta f$).

It may be shown [Ref. 83] that birefringent coherence is maintained over a length

of fiber L_{bc} (i.e. coherence length) when:

$$L_{bc} \simeq \frac{c}{B_F \delta f} = \frac{\lambda^2}{B_F \delta \lambda} \tag{3.59}$$

where c is the velocity of light in a vacuum and $\delta\lambda$ is the source linewidth.

However, when phase coherence is maintained (i.e. over the coherence length) Eq. (3.48) leads to a polarization state which is generally elliptical but which varies periodically along the fiber. This situation is illustrated in Figure 3.24(a) [Ref. 82] where the incident linear polarization which is at 45° with respect to the x axis becomes circular polarization at $\Phi = \pi/2$, and linear again at $\Phi = \pi$. The process continues through another circular polarization at $\Phi = 3\pi/2$ before returning to the initial linear polarization at $\Phi = 2\pi$. The characteristic length L_B corresponding to this process is known as the beat length. It is given by:

$$L_B = \frac{\lambda}{B_F} \tag{3.60}$$

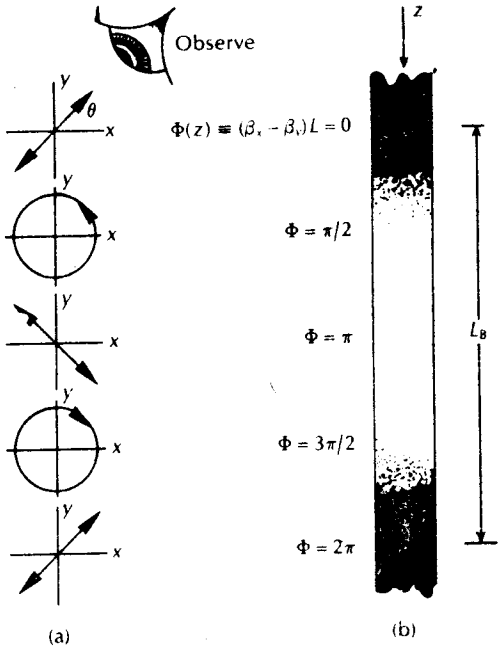

Figure 3.24 An illustration of the beat length in a single-mode optical fiber [Ref. 82]: (a) the polarization states against $\Phi(z)$; (b) the light intensity distribution over the beat length within the fiber.

Substituting for B_F from Eq. (3.47) gives:

$$L_B = \frac{2\pi}{(\beta_x - \beta_y)} \tag{3.61}$$

It may be noted that Eq. (3.61) may be obtained directly from Eq. (3.58) where:

$$\Phi(L_B) = (\beta_x - \beta_y)L_B = 2\pi \tag{3.62}$$

Typical single-mode fibers are found to have beat lengths of a few centimetres [Ref. 84], and the effect may be observed directly within a fiber via Rayleigh scattering with use of a suitable visible source (e.g. He–Ne laser) [Ref. 85]. It appears as a series of bright and dark bands with a period corresponding to the beat length, as shown in Figure 3.24(b). The modal birefringence B_F may be determined from these observations of beat length.

Example 3.12

The beat length in a single-mode optical fiber is 9 cm when light from an injection laser with a spectral linewidth of 1 nm and a peak wavelength of 0.9 μm is launched into it. Determine the modal birefringence and estimate the coherence length in this situation. In addition calculate the difference between the propagation constants for the two orthogonal modes and check the result.

Solution: To find the modal birefringence Eq. (3.60) may be used where:

$$B_F = \frac{\lambda}{L_B} = \frac{0.9 \times 10^{-6}}{0.09} = 1 \times 10^{-5}$$

Knowing B_F, Eq. (3.59) may be used to obtain the coherence length:

$$L_{bc} \simeq \frac{\lambda^2}{B_F \delta\lambda} = \frac{0.81 \times 10^{-12}}{10^{-5} \times 10^{-9}} = 81 \text{ m}$$

The difference between the propagation constant for the two orthogonal modes may be obtained from Eq. (3.61) where:

$$\beta_x - \beta_y = \frac{2\pi}{L_B} = \frac{2\pi}{0.09} = 69.8$$

The result may be checked by using Eq. (3.57) where:

$$\beta_x - \beta_y = \frac{2\pi B_F}{\lambda} = \frac{2\pi \times 10^{-5}}{0.9 \times 10^{-6}}$$

$$= 69.8$$

In a nonperfect fiber various perturbations along the fiber length such as strain or variations in the fiber geometry and composition lead to coupling of energy from

one polarization to the other. These perturbations are difficult to eradicate as they may easily occur in the fiber manufacture and cabling. The energy transfer is at a maximum when the perturbations have a period Λ, corresponding to the beat length, and defined by [Ref. 81]:

$$\Lambda = \frac{\lambda}{B_F} \tag{3.63}$$

However, the cross polarizing effect may be minimized when the period of the perturbations is less than a cutoff period Λ_c (around 1 mm). Hence polarization maintaining fibers may be designed by either:

1. High (large) birefringence: the maximization of the modal birefringence, which, following Eq. (3.60), may be achieved by reducing the beat length L_B to around 1 mm or less; or
2. Low (small) birefringence: the minimization of the polarization coupling perturbations with a period of Λ. This may be achieved by increasing Λ_c giving a large beat length of around 50 m or more.

Example 3.13

Two polarization maintaining fibers operating at a wavelength of 1.3 μm have beat lengths of 0.7 mm and 80 m. Determine the modal birefringence in each case and comment on the results.

Solution: Using Eq. (3.60), the modal birefringence is given by:

$$B_F = \frac{\lambda}{L_B}$$

Hence, for a beat length of 0.7 mm:

$$B_F = \frac{1.3 \times 10^{-6}}{0.7 \times 10^{-3}} = 1.86 \times 10^{-3}$$

This typifies a high birefringence fiber.

For a beat length of 80 m:

$$B_F = \frac{1.3 \times 10^{-6}}{80} = 1.63 \times 10^{-8}$$

which indicates a low birefringence fiber.

In a uniformly birefringent fiber, as mentioned previously, the orthogonal fundamental modes have different phase propagation constants β_x and β_y. Hence the two modes exhibit different specific group delays (see Section 2.5.4) of τ_{gx} and τ_{gy}. A delay difference $\delta\tau_g$ therefore occurs between the two orthogonally polarized

waves such that:

$$\delta\tau_g = \tau_{gx} - \tau_{gy} \tag{3.64}$$

where $\delta\tau_g$ is known as the polarization mode dispersion [Ref. 83]. Measured values of polarization mode dispersion range from significantly less than 1 ps km^{-1} in conventional single-mode fibers [Ref. 86] to greater than 1 ns km^{-1} in high birefringence polarization maintaining fibers [Ref. 87]. However, in specific low birefringence fibers, that is, spun fiber (see Section 3.13.2), polarization mode dispersion is negligible [Ref. 88].

Since the two fundamental modes generally launched into single-mode fiber have different group velocities, the output from a fiber length L will comprise two elements separated by a time interval $\delta\tau_g L$. For high birefringence fibers, the product $\delta\tau_g L$ provides a good estimate of pulse spreading in long fiber lengths. In this case the 3 dB bandwidth B is given by [Ref. 89]:

$$B = \frac{0.9}{(\delta\tau_g L)} \tag{3.65}$$

However, for short fiber lengths and fiber lengths longer than a characteristic coupling length L_c, the pulse spreading is proportional to $(LL_c)^{\frac{1}{2}}$ instead of simply L. Moreover, the maximum bit rate $B_T(\max)$ for digital transmission in relation to polarization mode dispersion may be obtained from [Ref. 90]:

$$B_T(\max) = \frac{B}{0.55} \tag{3.66}$$

Example 3.14

The polarization mode dispersion in a uniformly birefringent single-mode fiber is 300 ps km^{-1}. Calculate the maximum bit rate that may be obtained on a 20 km repeaterless link assuming only polarization mode dispersion to occur.

Solution: Combining Eqs. (3.65) and (3.66), the maximum bit rate is:

$$B_T(\max) = \frac{0.9}{0.55(\delta\tau_g)L} = \frac{0.9}{0.55 \times 300 \times 10^{-12} \times 20 \times 10^3}$$

$$= 273 \text{ kbit s}^{-1}$$

Although the maximum bit rate for the high birefringence fiber obtained in Example 3.14 is only 273 kbit s^{-1}, experimental results tend to indicate that polarization mode dispersion in long lengths of conventional single-mode fiber will not present a serious bandwidth limitation, even for systems operating to 1 Gbit s^{-1} with 100 km repeater spacings [Ref. 82]. For instance, measurement of polarization mode dispersion after cabling and jointing on an installed 30 km link was found to

be less than 0.5 ps [Ref. 92]. Nevertheless, polarization mode dispersion can cause intersymbol interference in digital optical fiber communication systems, or signal distortion in analog systems, known as polarization mode distortion.

Although certain single-mode fibers can be fabricated to propagate only one polarization mode (see Section 3.13.2), fibers which transmit two orthogonally polarized fundamental modes can exhibit interference between the modes which may cause polarization modal noise. This phenomenon occurs when the fiber is slightly birefringent and there is a component with polarization dependent loss. Hence, when the fiber link contains an element whose insertion loss is dependent on the state of polarization, then the transmitted optical power will depend on the phase difference between the normal modes and it will fluctuate if the transmitted wavelength or the birefringence alters. Any polarization sensitive loss will therefore result in modal noise within single-mode fiber [Ref. 93].

Polarization modal noise is generally of larger amplitude than modal noise obtained within multimode fibers (see Section 3.10.3). It can therefore significantly degrade the performance of a communication system such that high quality analog transmission may prove impossible [Ref. 51]. Moreover, with digital transmission it is usually necessary to increase the system channel loss margin (see Section 10.6.4). It is therefore important to minimize the use of elements with polarization dependent insertion losses (e.g. beam splitters, polarization selective power dividers, couplers to single polarization optical components, bends in high birefringence fibers) on single-mode optical fiber links. However, other types of fiber perturbation such as bends in low birefringence fibers, splices and directional couplers do not appear to introduce significant polarization sensitive losses [Ref. 81].

Techniques have been developed to produce both high and low birefringence fibers, initially to facilitate coherent optical communication systems. Birefringence occurs when the circular symmetry in single-mode fibers is broken which can result from the effect of geometrical shape or stress. Alternatively, to design low birefringence fibers it is necessary to reduce the possible perturbations within the fiber manufacture. These fiber types are discussed in the following section.

3.13.2 Polarization maintaining fibers

Although the polarization state of the light arriving at a conventional photodetector is not distinguished and hence of little concern, it is of considerable importance in coherent lightwave systems in which the incident signal is superimposed on the field of a local oscillator (see Section 12.3). Moreover, interference and delay differences between the orthogonally polarized modes in birefringent fibers may cause polarization modal noise and polarization mode dispersion respectively (see Section 3.13.1). Finally, polarization is also of concern when a single-mode fiber is coupled to a modulator or other waveguide device (see Section 10.6.2) that can require the light to be linearly polarized for efficient operation. Hence, there are several reasons why it may be desirable to use fibers that will permit light to pass through whilst

retaining its state of polarization. Such polarization maintaining (PM) fibers can be classified into two major groups: namely, high birefringence (HB) and low birefringence (LB) fibers.

The birefringence of conventional single-mode fibers is in the range $B_F = 10^{-6}$ to 10^{-5} [Ref. 88]. A HB fiber requires $B_F > 10^{-5}$ and a value better than 10^{-4} is a minimum for polarization maintenance [Ref. 94]. HB fibers can be separated into two types which are generally referred to as two-polarization fibers and single-polarization fibers. In the latter case in order to allow only one polarization mode to propagate through the fiber, a cutoff condition is imposed on the other mode by utilizing the difference in bending loss between the two polarization modes.

The various types of PM fiber, classified in terms of their linear polarization maintenance, are shown in Figure 3.25 [Ref. 95]. In addition, a selection of the most common structures is illustrated in Figure 3.26. The fiber types illustrated in Figure 3.26(a) and (b) employ geometrical shape birefringence, whilst Figure 3.26(c) to (g) utilize various stress effects. Geometrical birefringence is a somewhat weak effect and a large relative refractive index difference between the fiber core and cladding is required to produce high birefringence. Therefore, the elliptical core fiber of Figure 3.26(a) generally has high doping levels which tend to increase the optical losses as well as the polarization cross coupling [Ref. 96]. Alternatively, deep low refractive index side pits can be employed to produce HB fibers, as depicted in Figure 3.26(b).

Stress birefringence may be induced using an elliptical cladding (Figure 3.26(c)) with a high thermal-expansion coefficient. For example, borosilicate glass with some added germanium or phosphorus to provide index compensation can be utilized [Ref. 97]. The HB fibers shown in Figure 3.26(d) and (e) employ two distinct stress regions and are often referred to as the bow-tie [Ref. 98] and PANDA* [Ref. 99] fibers because of the shape of these regions. Alternatively, the flat cladding fiber design illustrated in Figure 3.26(f) has the outer edge of its elliptical cladding touching the fiber core which therefore divides the stressed cladding into two separate regions [Ref. 100].

In order to produce LB fibers attempts have been made to fabricate near-perfect, round-shaped core fibers. Ellipticity of less than 0.1% and modal birefringence of 4.5×10^{-9} has been achieved using the MCVD (see Section 4.4.3) fabricational technique [Refs. 101, 102]. Moreover, the residual birefringence within conventional single-mode fibers can be compensated for by twisting the fiber after manufacture, as shown in Figure 3.26(g). A twist rate of around five turns per metre is sufficient to reduce crosstalk significantly between the polarization modes [Ref. 95].

The reduction occurs because a high degree of circular birefringence is created by the twisting process. Hence, it is found that the propagation constants of the modes polarized in the left hand and right hand circular directions are different. This has the effect of averaging out the linear birefringence and thus produces a low

* The mnemonics PANDA, however, represent polarization maintaining and absorption reducing.

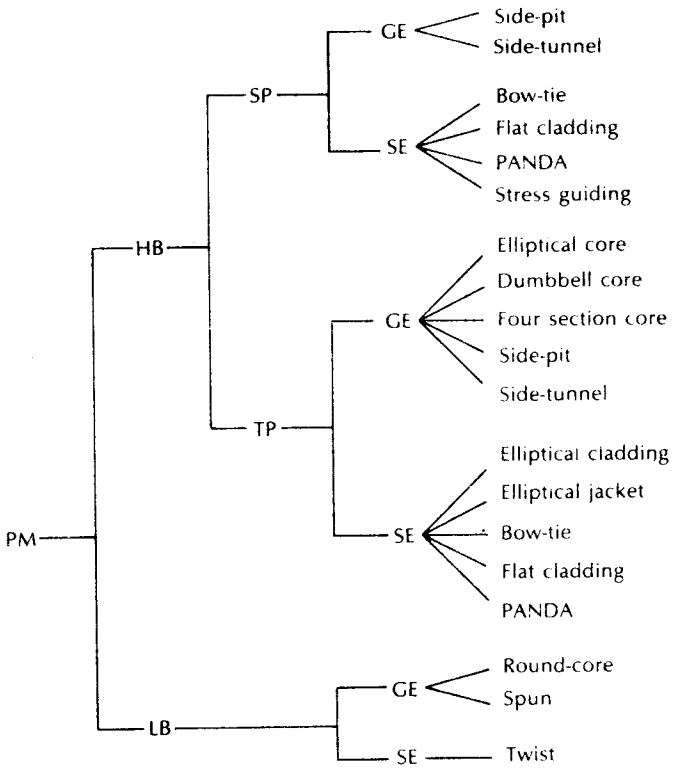

Figure 3.25 Polarization maintaining fiber types classified from linear polarization maintenance view point. PM: polarization maintaining, HB: high-birefringent, LB: low-birefringent, SP: single-polarization, TP: two-polarization modes, GE: geometrical effect, SE: stress effect [Ref. 95].

birefringence fiber. Unfortunately, the method has limitations as the fiber tends to break when beat lengths are reduced to around 10 cm [Ref. 104].

An alternative method of compensation for the residual birefringence in conventional circularly symmetric single-mode fibers is to rotate the glass preform during the fiber drawing process to produce spun fiber [Ref. 103]. This geometric effect also decreases the residual linear birefringence on average by introducing circular birefringence, but without introducing shear stress. The technique has produced fibers with modal birefringence as low as 4.3×10^{-9} [Ref. 95].

Another effective method of producing circularly birefringent fibers and thus reducing linear birefringence is to fabricate a fiber in which the core does not lie along the longitudinal fiber axis; instead the core follows a helical path about this axis [Ref. 105]. To obtain such fibers a normal MCVD (see Section 4.4.3) preform containing core and cladding glass is inserted into an off-axis hole drilled in a silica

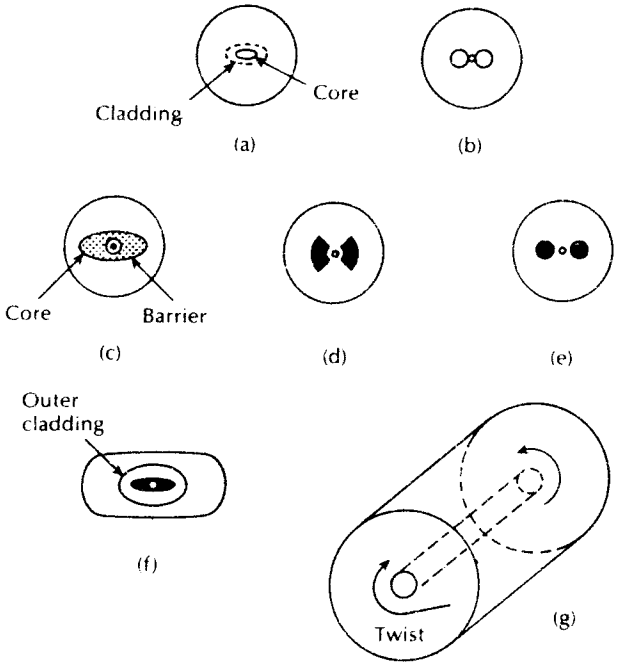

Figure 3.26 Polarization maintaining fiber structure; (a) elliptical core; (b) side-pit fiber; (c) elliptical stress-cladding; (d) bow-tie stress regions; (e) circular stress regions (PANDA fiber); (f) flat fiber; (g) twisted fiber.

rod. Then as the silica rod containing the offset core–cladding preform is in the process of being drawn into fiber, it is rotated about its longitudinal axis. The resulting fiber core forms a tight helix which has a pitch length of a few millimetres. In this case the degree of circular birefringence tends to be an order of magnitude or more greater than that achieved by twisting the fiber, giving beat lengths of around 5 mm or less.

The characteristics of the aforementioned PM fibers are not only described by the modal birefringence or beat length but also by the mode coupling parameters or polarization crosstalk as well as their transmission losses. The mode coupling parameter or coefficient h, which characterizes the polarization maintaining ability of fibers based on random mode coupling, proves useful in the comparison of different lengths of PM fiber. It is related to the polarization crosstalk* CT by [Ref 95]:

$$CT = 10 \log_{10} \frac{P_y}{P_x} = 10 \log_{10} \tanh(hL) \tag{3.67}$$

* The crosstalk is also referred to as the extinction ratio at the fiber output between the unwanted mode and the launch mode.

where P_x and P_y represent the optical power in the excited (i.e. unwanted) mode and the coupled (i.e. launch) mode, respectively, in an ensemble of fiber length L. However, it should be noted that the expression given in Eq. (3.67) applies with greater accuracy to two-polarization fibers because the crosstalk in a single polarization fiber becomes almost constant around -30 dB and is independent of the fiber length beyond 200 m [Ref. 106].

Example 3.15

A 3.5 km length of two polarization mode PM fiber has a polarization crosstalk of -27 dB at its output end. Determine the mode coupling parameter for the fiber.

Solution: Using Eq. (3.67) relating the mode coupling parameter h to the polarization crosstalk CT:

$$\log_{10} \tanh (hL) = \frac{CT}{10} = -2.7$$

Thus $\tanh (hL) = 2 \times 10^{-3}$ and $hL \simeq 2 \times 10^{-3}$

Hence $$h = \frac{2 \times 10^{-3}}{3.5 \times 10^{3}} = 5.7 \times 10^{-7}\ \text{m}^{-1}$$

The generally higher transmission losses exhibited by PM fibers over conventional single-mode fibers is a major consideration in their possible utilization within coherent optical fiber communication systems. This factor is, however, less important when dealing with the short fiber lengths employed in fiber devices (see Section 5.6). Nevertheless, care is required in the determination of the cutoff wavelength or the measurement of fiber loss at longer wavelengths than cutoff because the transmission losses of the HE_{11}^{x} and HE_{11}^{y} modes in HB fibers exhibit different wavelength dependencies. PM fibers with losses approaching those of conventional single-mode fiber have been fabricated recently. For example, optical losses of around 0 23 dB km^{-1} at a wavelength of 1.55 μm with polarization crosstalk of -36 dB km^{-1} have been obtained [Refs. 107, 108]. Such PM fibers could therefore eventually find application within long-haul coherent optical fiber transmission systems.

3.14 Nonlinear phenomena

Although the initial work concerned with nonlinear optical effects used relatively large core multimode fibers, more recently such phenomena have become very important within the development of low loss, single-mode fibers [Ref. 106]. The small core diameters, together with the long propagation distances that may be

obtained with these fibers, has enabled the observation of certain nonlinear phenomena at power levels of a few milliwatts which are well within the capability of semiconductor lasers. Fiber attenuation associated with nonlinear scattering was discussed in Section 3.5 but these and other nonlinear processes may also be employed in important applications of single-mode fibers.

Interest has grown in the use of fibers as an interaction medium for stimulated Brillouin and Raman scattering as well as self phase modulation and four-wave mixing. The latter process, however, requires at least two propagating modes in order to fulfil the associated phase matching conditions, unless it takes place around the zero chromatic dispersion wavelength [Ref. 109]. In this section we will therefore concentrate on the other phenomena and their effects within single-mode fibers.

It was indicated in Section 3.5 that when an optical wave is within a fiber medium incident photons may be scattered, producing a phonon emitted at acoustic frequencies by exciting molecular vibrations, together with another photon at a shifted frequency. In quantum mechanical terms this process can be described as the molecule absorbing the photon at the original frequency whilst emitting a photon at the shifted frequency and simultaneously making a transition between vibrational states. The scattered photon therefore emerges at a frequency shifted below or above the incident photon frequency with the energy difference between the two photons being deposited or extracted from the scattering medium. An upshifted photon frequency is only possible if the material gives up quantum energy equal to the energy difference between the incident and scattered photon. The material must therefore be in a thermally excited state before the incident photon arrives, and at room temperature (i.e. 300 K) the upshifted scattering intensity is much weaker than the downshifted one. The former scattered wave is known as the Stokes component whereas the latter is referred to as the anti-Stokes component. In contrast to linear scattering (i.e. Rayleigh), which is said to be elastic because the scattered wave has the same frequency as the incident wave, these nonlinear scattering processes are clearly inelastic. A schematic of the spectrum obtained from these inelastic scattering processes is shown in Figure 3.27. It should be noted that the schematic depicts the spontaneous scattering spectrum rather than the stimulated one.

The frequency shifts associated with inelastic scattering can be small (less than $1\ \text{cm}^{-1}$), which typifies Brillouin scattering with an acoustic frequency phonon. Larger frequency shifts (greater than $100\ \text{cm}^{-1}$) characterize the Raman regime where the photon is scattered by local molecular vibrations or by optical frequency phonons. An interesting feature of these inelastic scattering processes is that they not only result in a frequency shift but for sufficiently high incident intensity they provide optical gain at the shifted frequency. The incident optical frequency is also known as the pump frequency ω_p, which gives the Stokes (ω_s) and anti-Stokes (ω_a) components of the scattered radiation (see Figure 3.27). For a typical fiber, a pump power of around one watt in 100 m of fiber results in a Raman gain of about a factor of 2 [Ref. 110]. By contrast, the peak Brillouin gain is more than two orders

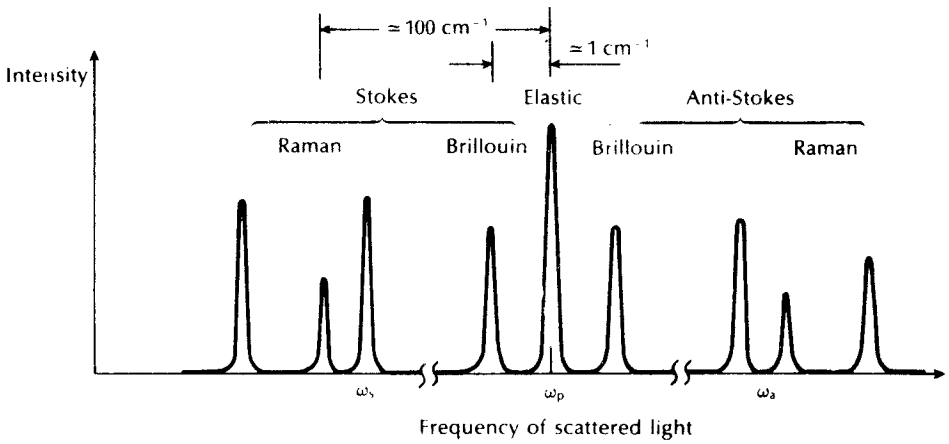

Figure 3.27 Spectrum of scattered light showing the inelastic scattering processes. Not drawn to scale as the intensities of the anti-Stokes Raman lines are far less than those of the Stokes Raman lines.

of magnitude greater than the Raman gain, but the Brillouin frequency shift and gain bandwidth are much smaller. Furthermore, Brillouin gain only exists for light propagation in the opposite direction to the pump light whilst Raman amplification will occur for light propagating in either direction.

Raman gain also extends over a substantial bandwidth, as may be observed in Figure 3.28 [Ref. 111]. Hence, with a suitable pump source, a fiber can function as a relatively high gain, broad bandwidth, bidirectional optical amplifier (see Section 10.4.2). Although given its much greater peak gain, it might be expected that Brillouin amplification would dominate over Raman amplification. At present this is not usually the case because of the narrow bandwidth associated with the Brillouin process which is often in the range 20 to 80 MHz. Pulsed semiconductor laser sources generally have much broader bandwidths and therefore prove inefficient pumps for such a narrow gain spectrum.

Nonlinear effects which can be readily described by the intensity dependent refractive index of the fiber are commonly referred to as Kerr nonlinearities. The refractive index of a medium results from the applied optical field perturbing the atoms or molecules of the medium to induce an oscillating polarization, which then radiates, producing an overall perturbed field. At low intensities the polarization is a linear function of the applied field and hence the resulting perturbation of the field can be realistically described by a constant refractive index. However, at higher optical intensities the perturbations do not remain linear functions of the applied field and Kerr nonlinearities may be observed. Typically, in the visible and infrared wavelength regions Kerr nonlinearities do not exhibit a strong dependence on the frequency of the incident light because the resonant frequencies of the oscillations tend to be in the ultraviolet region of the spectrum [Ref. 112].

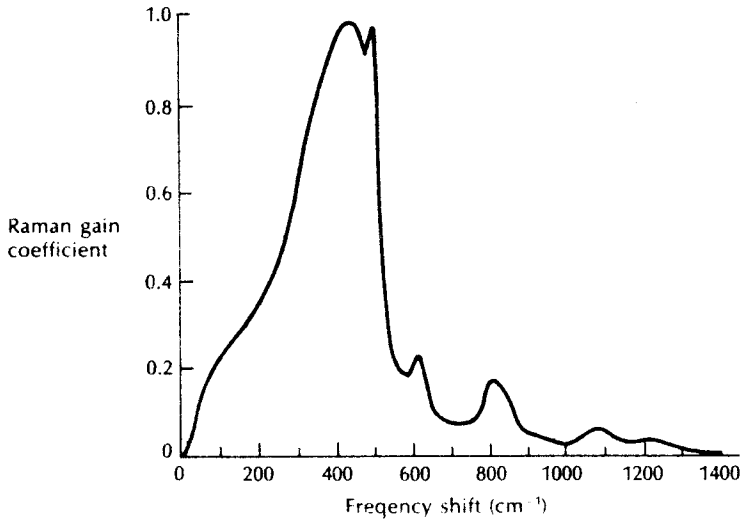

Figure 3.28 Raman gain spectrum for a silica core single-mode fiber. The peak gain occurred at 440 cm^{-1} with a pump wavelength of 0.532 μm. Reproduced with permission from W. J. Tomlinson and R. H. Stolen 'Nonlinear phenomena in optical fibers', *IEEE Commun. Mag.*, **26**, p. 36, 1988. Copyright © 1988 IEEE.

The intensity dependent refractive index causes an intensity dependent phase shift in the fiber. Hence, for a light pulse propagating in the fiber, Kerr nonlinearities result in a different transmission phase for the peak of the pulse compared to the leading and trailing pulse edges. This effect, which is known as self phase modulation, causes modifications to the pulse spectrum. As the instantaneous frequency of a wave is the time derivative of its phase, then a time-varying phase creates a time-varying frequency. Thus self phase modulation can alter and broaden the frequency pectrum of the pulse. In addition to self phase modulation, or the alteration of the pulse by itself, Kerr nonlinearities also allow a pulse to be modified by another pulse which can be at a different polarization or alternatively just a different mode of the fiber.

Although self phase modulation can simply be used for frequency shifting [Ref. 113], it has found major application for pulse compression within single-mode fiber transmission [Refs. 108 to 110]. In this context self phase modulation effectively imposes a chirp, or positive frequency sweep, on the pulse. This phenomenon combined with the group-velocity dispersion* occurring within the fiber allows

* It is usual to describe the group-velocity dispersion resulting from the frequency dependence of the group velocity (i.e. the different spectral components within a pulse exhibit a different group delay τ_g thus causing pulse spread) in terms of the intramodal or chromatic dispersion which for a unit length of fiber is defined by $d\tau_g/d\lambda$.

optical pulses to be compressed by employing, for example, a pair of diffraction gratings in which the longer wavelength light travelling at the front of the pulse follows a longer path length than the shorter wavelength light at the rear of the pulse. Hence, the rear of the pulse catches up with the front of the pulse and compression occurs. Furthermore, for critical pulse shapes and at high optical power levels, such pulse compression can be obtained in the fiber itself which forms the basis of so-called soliton propagation [Ref. 114]. Such nonlinear pulses can propagate without any dispersive changes (i.e. their shapes are self maintaining) and hence they are of great interest for communications [Ref. 110]. However, since soliton propagation is the result of a nonlinear phenomenon, it is critically dependent on the intensity of the pulse. Unfortunately, even with low loss fibers, a soliton propagating along a fiber will gradually lose energy and hence its special characteristics. Nevertheless, strategies to overcome this drawback are under investigation [e.g. Ref. 115].

Problems

3.1 The mean optical power launched into an optical fiber link is 1.5 mW and the fiber has an attenuation of 0.5 dB km^{-1}. Determine the maximum possible link length without repeaters (assuming lossless connectors) when the minimum mean optical power level required at the detector is 2 μW.

3.2 The numerical input/output mean optical power ratio in a 1 km length of optical fiber is found to be 2.5. Calculate the received mean optical power when a mean optical power of 1 mW is launched into a 5 km length of the fiber (assuming no joints or connectors).

3.3 A 15 km optical fiber link uses fiber with a loss of 1.5 dB km^{-1}. The fiber is jointed every kilometre with connectors which give an attenuation of 0.8 dB each. Determine the minimum mean optical power which must be launched into the fiber in order to maintain a mean optical power level of 0.3 μW at the detector.

3.4 Discuss absorption losses in optical fibers, comparing and contrasting the intrinsic and extrinsic absorption mechanisms.

3.5 Briefly describe linear scattering losses in optical fibers with regard to:

(a) Rayleigh scattering;
(b) Mie scattering.

The photoelastic coefficient and the refractive index for silica are 0.286 and 1.46 respectively. Silica has an isothermal compressibility of 7×10^{-11} m^{2}N^{-1} and an estimated fictive temperature of 1400 K. Determine the theoretical attenuation in decibels per kilometre due to the fundamental Rayleigh scattering in silica at optical wavelengths of 0.85 and 1.55 μm. Boltzmann's constant is 1.381×10^{-23} J K^{-1}.

3.6 A K_2O–SiO_2 glass core optical fiber has an attenuation resulting from Rayleigh scattering of 0.46 dB km^{-1} at a wavelength of 1 μm. The glass has an estimated fictive temperature of 758 K, isothermal compressibility of 8.4×10^{-11} m^{2}N^{-1}, and a photoelastic coefficient of 0.245. Determine from theoretical considerations the refractive index of the glass.

3.7 Compare stimulated Brillouin and stimulated Raman scattering in optical fibers, and indicate the way in which they may be avoided in optical fiber communications.

The threshold optical powers for stimulated Brillouin and Raman scattering in a long 8 μm core diameter single-mode fiber are found to be 190 mW and 1.70 W, respectively, when using an injection laser source with a bandwidth of 1 GHz. Calculate the operating wavelength of the laser and the attenuation in decibels per kilometre of the fiber at this wavelength.

3.8 The threshold optical power for stimulated Brillouin scattering at a wavelength of 0.85 μm in a long single-mode fiber using an injection laser source with a bandwidth of 800 MHz is 127 mW. The fiber has an attenuation of 2 dB km^{-1} at this wavelength. Determine the threshold optical power for stimulated Raman scattering within the fiber at a wavelength of 0.9 μm assuming the fiber attenuation is reduced to 1.8 dB km^{-1} at this wavelength.

3.9 Explain what is meant by the critical bending radius for an optical fiber.

A multimode graded index fiber has a refractive index at the core axis of 1.46 with a cladding refractive index of 1.45. The critical radius of curvature which allows large bending losses to occur is 84 μm when the fiber is transmitting light of a particular wavelength. Determine the wavelength of the transmitted light.

3.10 A single-mode step index fiber with a core refractive index of 1.49 has a critical bending radius of 10.4 mm when illuminated with light at a wavelength of 1.30 μm. If the cutoff wavelength for the fiber is 1.15 μm calculate its relative refractive index difference.

3.11 (a) A multimode step index fiber gives a total pulse broadening of 95 ns over a 5 km length. Estimate the bandwidth–length product for the fiber when a nonreturn to zero digital code is used.

(b) A single-mode step index fiber has a bandwidth–length product of 10 GHz km. Estimate the rms pulse broadening over a 40 km digital optical link without repeaters consisting of the fiber, and using a return to zero code.

3.12 An 8 km optical fiber link without repeaters uses multimode graded index fiber which has a bandwidth–length product of 400 MHz km. Estimate:

(a) the total pulse broadening on the link;
(b) the rms pulse broadening on the link.

It may be assumed that a return to zero code is used.

3.13 Briefly explain the reasons for pulse broadening due to material dispersion in optical fibers.

The group delay τ_g in an optical fiber is given by:

$$\tau_g = \frac{1}{c}\left(n_1 - \frac{\lambda \mathrm{d}n_1}{\mathrm{d}\lambda}\right)$$

where c is the velocity of light in a vacuum, n_1 is the core refractive index and λ is the wavelength of the transmitted light. Derive an expression for the rms pulse broadening due to material dispersion in an optical fiber and define the material dispersion parameter.

The material dispersion parameter for a glass fiber is 20 ps nm^{-1} km^{-1} at a wavelength of 1.5 μm. Estimate the pulse broadening due to material dispersion within the fiber when light is launched from an injection laser source with a peak wavelength of 1.5 μm and an rms spectral width of 2 nm into a 30 km length of the fiber.